UNIVERSITY OF TRENTO

International PhD Program in Biomolecular Sciences

30th Cycle

"Cell-free expression systems for the construction of artificial cells"

Tutor

Professor Sheref S. Mansy

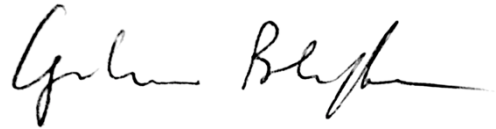*Cibio – University of Trento*

Ph.D. Thesis of

Giuliano Berloffa

CIBIO – University of Trento

Academic Year 2016 - 2017

I, Giuliano Berloffa, confirm that this is my own work and the use of all material from other sources has been properly and fully acknowledged.

Abstract

Cell-free expression systems are widely used to synthesize proteins for subsequent further characterization, to manufacture potentially useful commercial end products, and to construct cellular mimics in the laboratory. The first part of the thesis explores the feasibility of preparing two of the commercially available and widely used *E. coli*-based cell-free expression systems: the PURE System and the S30 Bacterial Extract. The second part focuses on the characterization of *in vitro* transcription and translation. The third part of the thesis features an example of an application of S30 Bacterial Extract cell-free expression systems *i.e.* the building of cell-like structures that can work together with engineered bacteria to achieve a predetermined task. Finally, the construction of a microfluidic dialysis device compatible with cell-free synthetic biology projects is presented.

Contents

Introduction

The regulation and control of living systems behavior have always represented a major concern and interest for mankind. Some of the most crucial steps in the development of modern society are due to the successful control of biological entities neighboring the human beings, see the outbreak of agriculture and livestock breeding. More sophisticated techniques for the control of living systems have evolved together with the increase of knowledge of the systems themselves. As an example, understanding how plants work allowed to develop grafting procedures for the creation of more productive and resistant cultivars and crossbreeding was introduced to obtain the same result for livestock.

With the beginning of the biotechnology era, the control of living systems deepened to the cellular level. Attempts to control cellular behavior are mainly based on genetic engineering. This approach is definitely useful and allows to achieve unprecedented results. Nevertheless, a comprehensive and ample understanding on how living cell function is far to be fully achieved. This knowledge limitation may translate in the arise of unwanted or unexpected traits since living cells can grow, evolve and eventually modify the engineered circuits. The creation of completely new entities with only specific and desired cell functions would lead to controlled and programmable cellular mimics, a solution to the unpredictability of engineered natural systems. Natural cells regulate their behavior by sensing and responding to the surrounding environmental changes and to other cells signaling. Artificial systems can be built and designed to interact with natural communication pathways with the desired result of taking active part in cellular communication and effectively modify cellular behavior. Moreover, attempts to modify behavior of cells through the mimicking of natural communication may lead to a better understanding of how such systems function. Two main approaches are employed for the synthesis of artificial cells, top-down and bottom-up. The top-down approach aims to achieve a minimal system driven by an essential gene set by depleting unwanted functions from pre-existing cells. The bottom-up approach starts with the creation of a cell-like system from minimal non-living components. The resulting artificial cell consists of the basic elements that are usually associated with natural cells, such as *i)* a compartment for the isolation of the interior from the surrounding environment, *ii)*

information about the function of the system, usually encoded into nucleic acids, *iii)* a machinery that can interpret the information and translate it into a desired output.

This work focuses on cell-free protein expression systems which may constitute the interior machinery of artificial cells. Cell-free protein expression systems can be prepared in different ways and can be based on diverse host organism but share the common feature of lacking the host genetic information. The desired function can be given to an artificial cell by encapsulating cell-free protein expression system provided with a specific template, thus allowing for the synthesis of one or more desired proteins.

The first chapter focuses on the exploration of two of the most popular *E. coli* based cell-free expression systems. These systems were prepared in the lab and tested for activity. Here, an attempt to reconstitute the PURE, a contaminant-free system built with purified components only, is presented and the successful reconstitution of *E. coli* S30 Extract is shown. In the second chapter cell-free expression systems are used to characterize *in vitro* transcription and translation. The work presented provides evidences that *in vitro* translation is more variable than transcription and that this is at least partially due to the higher system complexity of translation compared to transcription and the GC content and mRNA. The third chapter describes one step towards the establishment of artificial cells communities. A known issue of artificial cells is the depletion of energy resources which constitutes a limitation in the lasting and efficacy of such systems. Here, is presented the characterization of one step of a proposed network of artificial and engineered cells, for the proof-of-concept that energy-expensive tasks could be eventually completed by a consortium of different artificial cells. The last chapter of the thesis presents the construction of a microfluidics dialysis device. The preparation of a part of the platform was characterized and the resulting platform was used to perform and monitor chemical communication among engineered bacteria and among cell-free reactions. The dialysis chip could eventually be exploited for testing and prototyping genetic circuits for cell-free protein expression systems of for the characterization of uncultured microorganisms.

Chapter 1.

Homemade cell-free expression systems

1.1. Introduction

One of the most important discoveries in molecular biology was that lysates from shredded bacteria or cells could still provide evidences of occurring protein synthesis. Rapidly, cell-free or *in vitro* protein synthesis systems were developed by removal of the heavier components by centrifugation at 30,000 x*g*, the S30 Extracts.

The first reports of cell-free protein synthesis were mainly studies of the mechanisms at the core of translation. The investigation of how amino acids are incorporated into nascent polypeptides was indeed tackled in the early 50s and mostly featured cell-free expression systems based on different organisms. Among the others, systems based on rat liver cells[1], bacteria[2,3], human and rabbit reticulocites[4,5] allowed for the discovery of the key role of ribosomes and the ATP- and GTP-dependent operation of protein synthesis[6,7]. At that time, designing protein expression experiments with cell-free systems was more appealing than working *in vivo*, as recombinant DNA technologies and genetic engineering protocols were not available until some decades later[8,9]. One of the most remarkable achievements using cell-free expression systems was the finding of amino acids codification in nucleotide triplets. In 1961 Nirenberg and Matthaei, awarded with the Nobel Prize in Medicine a few years later, demonstrated cell-free synthesis of polyphenylalanine from synthetic polyuridylic acid in the *E. coli* extract[10]. Described in this work there is also one of the first reports of translation of exogenous message after the removal of all endogenous mRNA.

As a result of the breakout of recombinant DNA tools, cell-free expression lost part of the attention and working *in vivo* using cellular or bacterial hosts became prevalent, both for basic research and for protein production. Exception was made for some application niches in which *in vitro* protein synthesis was still preferred, for example for the production of hard-to-express proteins such as antibodies[11,12] or cytotoxic proteins[13,14]. Despite the predominance of *in vivo* technologies in terms of scale and ease

of procedures, another major step was taken towards more efficient *in vitro* systems. The introduction of coupled transcription-translation cell-free systems allowed to prime the protein production reaction with DNA, rather than using mRNA[15]. This breakthrough not only simplified the protocol, bypassing the initial *in vitro* transcription step, but also opened new possibilities for the study of gene regulation.

Innovation continued with the introduction of heterologous systems which combined the high processivity of bacteriophage RNA polymerases with the previously mentioned translation machineries. SP6 RNA polymerase and T7 RNA polymerase[16,17] were employed for driving the specific transcription of genes placed behind the correspondent promoter with several advantages. In bacteria-based extract, the selective inhibition of endogenous RNA polymerase by the addition of rifampicin[18] allows for highly selective expression of the protein of interest. Moreover, the mRNA levels provided by phage RNA polymerases are higher than the ones obtained with endogenous polymerases[19].

In 2001, the issues related to inhibitory factors and residual synthesis of non-specific endogenous proteins were addressed by the Ueda group with the creation of the PURE system (Protein synthesis Using Recombinant Elements)[20]. The PURE system features *i)* the full set of components required for efficient protein synthesis *i.e* the 20 tRNA synthetases (ARSs), 3 translation initiation factors (IF1, IF2, and IF3), 3 translation elongation factors (EF-G, EF-Tu, and EFTs), 3 translation termination factors (RF1, RF2, and RF3), methionyl-tRNA transformylase (MTF), T7 RNA polymerase, and ribosomes; *ii)* the substrate molecules needed for efficient transcription and translation reactions to occur *i.e.* 46 transfer RNAs (tRNAs), ribonucleotides (NTPs), 10-formyl-5,6,7,8-tetrahydrofolic acid (folinic acid) and 20 amino acids; *iii)* an energy storage system based on ATP regeneration and side products disposal *i.e.* creatine phosphate, creatine kinase, myokinase, nucleoside-diphosphate kinase, and pyrophosphatase.

The PURE system, free of unnecessary cellular components, facilitates *in vitro* studies thanks to a much cleaner background than a lysate-based system. The absence of nucleases ensures a higher stability of the DNA template and the mRNA, allowing the use of linear DNA templates. The PURE system showed to fit the needs of *in vitro* protein engineering[21] and performed well in such *in vitro* applications as mRNA display[22] and

ribosome display[23,24]. The highly controlled content of the system allows also for its customization for the expression of proteins which require particular folding conditions. The addition of glutathione, disulfide isomerase and chaperons to the system specifically meant for protein disulfide bonds enhancement[21,25] whereas the implementation with membrane integration/translocation systems led to the successful expression and folding of integral membrane proteins[26]. Another well-covered advantage in using the PURE system is the possibility to omit one of the release factors (RF1) for the incorporation of un-natural amino acids at specific amber codon sites (UAG) using chemically mis-acylated suppressor tRNA[20,27–29].

The great limitation in the use of the PURE system is the lack of proteins which could help the efficiency of protein translation[30] or the complete maturation of products that need post-translational modification. It was shown that adding some of the major *E. coli* molecular chaperones to the *in vitro* PURE system reaction was enough to rescue the folding and to increase the production yield of many aggregation-prone cytosolic *E. coli* proteins[31]. Moreover, it is not ruled out the likelihood that the PURE system lacks some other unknown factors aiding the fully translation and folding of active globular proteins, leading also to a narrow temperature range of optimal operation in comparison to the more flexible extracts. The addition of the heterogeneous S30 *E. coli* crude lysate to the PURE system reaction was indeed observed to improve the yield and activity of synthesized heterologous enzymes even at lower reaction temperature when usually the PURE system is not quite performing[32]. Finally, the high expenses of using commercial PURE system cannot be neglected. Currently sold by New England Biolabs, "PURExpress *In Vitro* Protein Synthesis Kit" has a cost per µL 8-fold higher than homemade S30 *E. coli* Extract[33]. The entire protocol for reconstituting the PURE system in the lab has been published[34] and accounts for the preparation of the >100 components reaction. A simpler approach was proposed by the Church lab which genetically modified the genome of *E. coli* to constitutively express a His-tagged version of all the translation factors and tRNA synthetases[35].

Cell-free protein synthesis for the construction of artificial cells

Cell-free protein synthesis is the natural starting point for any bottom-up approach to the creation of an artificial cell as opposed. Indeed, a large part of the essential genes believed to be sufficient for the sustainment of a living bacterium are involved in protein synthesis[36]. Although a completely bottom-up viable artificial cell has not yet been delivered, cell-free protein synthesis has successfully been performed in phospholipid vesicles[37,38] and water-in-oil droplets[39] also to establish working communication with natural and engineered cells[40,41]. In light of the key role of cell-free protein systems in powering the first functioning synthetic cell entities, it becomes clear how the study and development of these tools are essential for bottom-up reconstruction of the minimal cell[42,43]. Numerical modelling approaches has also been shown to provide a valuable resource for the characterization of compartmentalization efficiency[44] and cell-free transcription-translation systems output[45].

Here are presented three attempts to achieve a performing *in vitro* protein synthesis system by reconstituting: *a)* the homemade version of the PURE, assembled according to Ueda's instructions[34]; *b)* another homemade version of the PURE, prepared following Church's approach[35] *i.e.* by purifying pools of enzymes instead of performing many individual purifications; *c)* the homemade S30 *E. coli* Extract described by Noireaux[33].

1.2. Results

To obtain more flexibility on template choice and transcription-translation levels in the reconstituted PURE system, both T7 and *E. coli* RNA polymerases were purified. Indeed, T7 RNA polymerase is well known for its high processivity and efficiency, while *E. coli* RNA polymerase can drive transcription from a wide set of promoters with different levels of activity.

T7 RNA polymerase cloning, purification and test

T7 RNA polymerase was cloned, overexpressed and purified to drive the transcription of genes controlled by a T7 promoter in the homemade PURE system reaction. T7 RNA polymerase coding sequence and backbone were amplified by PCR using Phusion DNA polymerase (New England Biolabs) from TargeTron™ Vector pAR1219 (Sigma) and pET21b (Addgene) respectively. T7 polymerase coding sequence was cloned into pET21b plasmid by Gibson Assembly. His-tagged T7 RNA polymerase was overexpressed and purified as described in the Material and methods section. The presence of purified protein in the elution fractions was assessed by SDS-PAGE (Figure 1) and fractions 8 to 13 were pooled and dialyzed against storage buffer. Purified T7 RNA polymerase activity was assessed by performing an *in vitro* transcription reaction (Figure 2). Plasmid template used for the reaction was FC001A carrying the coding sequence of malachite green aptamer (MGA)[44] under the transcriptional regulation of T7 promoter. MGA RNA folds in a secondary structure reconstituting a fluorophore. Binding to malachite green strongly increases the quantum yield of the fluorophore allowing for indirect monitoring of the transcribed RNA levels. Malachite green aptamer fluorescence was monitored in real time by fluorescence spectroscopy using Rotor-Gene Q 6plex (Qiagen).
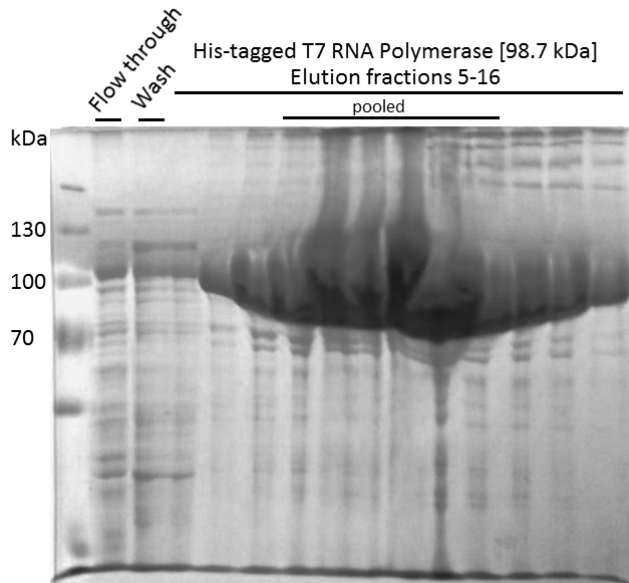
Figure 1. His-tagged T7 RNA polymerase Ni^{++} affinity chromatography purification SDS-PAGE. *Lane 1: PageRuler Plus Protein Ladder (Thermo Fisher Scientific); lane 2: flow through; lane 3: wash; lanes 4 through 15: elution fractions 5 through 16. His-tagged T7 RNA polymerase expected mass is 100 kDa. Pooled fractions: 8 through 13.*
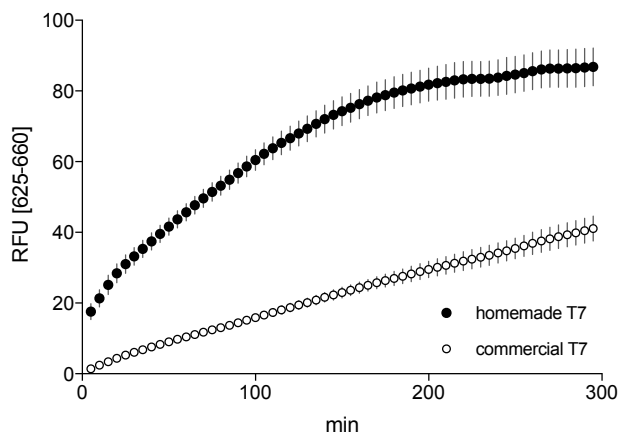
Figure 2. T7 RNA polymerase activity test. *His-tagged T7 RNA polymerase function was tested in an in vitro transcription reaction using FC001A plasmid as template. FC001A carries malachite green aptamer coding sequence under transcription regulation of T7 promoter. Commercial T7 RNA polymerase (New England Biolabs) was used as a positive control. RNA polymerase amount used in the in vitro reaction was 1/10 of the reaction volume as recommended in commercial T7 manual. Reactions were run in duplicate at 37 °C and malachite green fluorescence data was acquired with Rotor-Gene Q 6plex (Qiagen) (excitation: 625±5 nm; emission: 660±10 nm)*

The preparation of T7 RNA polymerase yielded a sub-homogeneous stock. The purified His-tagged protein seemed more efficient compared to the commercial T7 RNA polymerase, using the malachite green aptamer detection system. In fact, using the same amount of enzyme recommended by the manufacturer, fluorescence was 2-fold higher.

E. coli RNA polymerase, σ^{70} purification and test

E. coli RNA polymerase and σ^{70} were overexpressed and purified to be reconstituted in the homemade PURE system in order to drive the transcription of genes under the regulation of constitutive E. coli promoter or different promoters recognized by E. coli RNA polymerase, such as T5 promoter.

His-tagged E. coli RNA polymerase core enzyme was prepared in three purification steps. First by benchtop Ni^{++} affinity chromatography, then by Heparin affinity chromatography and finally by ion-exchange chromatography using Äkta FPLC (GE Healthcare). SDS-PAGE was run to assess the content of elution fractions after each purification step. In particular elution fractions of ion-exchange chromatography are shown in Figure 3.
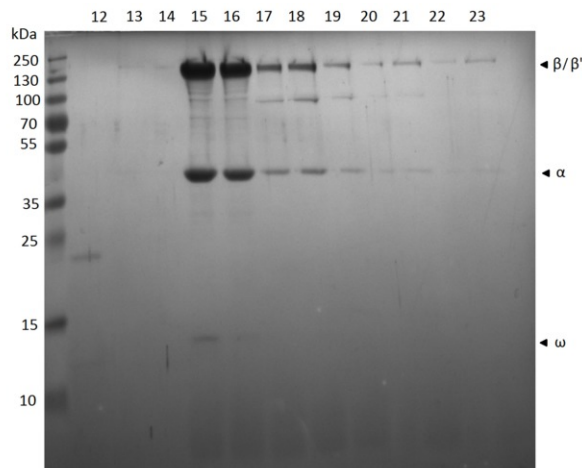
Figure 3. His-tagged E. coli RNA polymerase core enzyme ion exchange chromatography purification SDS-PAGE. Lane 1: PageRuler Plus Protein Ladder (Thermo Fisher Scientific); lane 2 through 14: elution fractions 12 through 23. His-tagged E. coli RNA polymerase subunits have expected masses of: 36.5 kDa (α), 150.6 kDa (β), 155.1 kDa (β'), 10.2 kDa (ω). Pooled fractions: 15 through 18.

SDS-PAGE shows that the three purification steps allowed for a quasi-homogeneous preparation of *E. coli* RNA polymerase core enzyme.

His-tagged σ^{70} transcription factor was prepared in two purification steps. First by benchtop Ni^{++} affinity chromatography then by ion-exchange chromatography using Äkta FPLC (GE Healthcare). SDS-PAGE was run to assess the content of elution fractions after each purification step. In particular elution fractions of ion-exchange chromatography are shown in Figure 4.
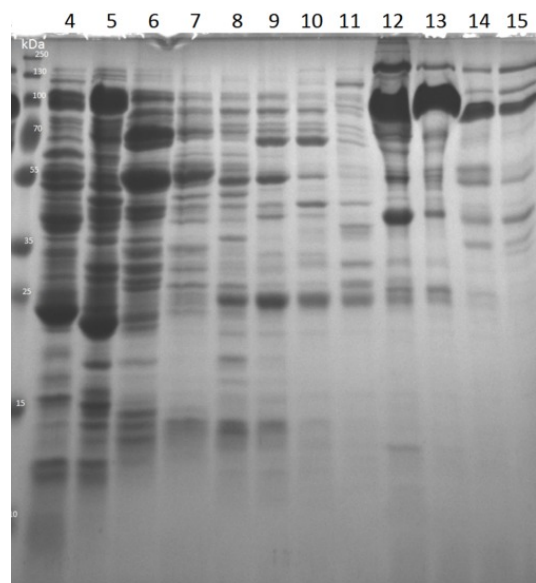
Figure 4. His-tagged σ^{70} transcription factor ion exchange chromatography purification SDS-PAGE. *Lane 1: PageRuler Plus Protein Ladder (Thermo Fisher Scientific); lanes 2 through 13: elution fractions 4 through 15. His-tagged σ^{70} transcription factor has expected mass of: 36.5 kDa (α), 150.6 kDa (β), 155.1 kDa (β'), 10.2 kDa (ω). Pooled fractions: 12 through 14.*

SDS-PAGE shows that the two purification steps yielded a sub-homogeneous stock of σ^{70} transcription factor.

The activity of the reconstituted *E. coli* RNA polymerase was assessed in *in vitro* transcription reaction exploiting the malachite green aptamer detection system (Figure 5). Templates were two plasmids carrying the coding sequence of MGA downstream of RFP under the transcription regulation of the *E. coli* promoter pTac. One of the two plasmids

carries the MGA sequence located in a bigger aptamer, called pRNA, which is specifically designed for enhancing and protecting the structure of the hosted aptamers[45]. By testing various concentrations and combinations of the core enzyme and σ^{70} factor, it was possible to determine the best performing ratio of the core to σ^{70} factor to be 1:2.5. Optimal working concentrations are shown in Table 1. In this condition, the reconstituted *E. coli* RNA holoenzyme performed better in *in vitro* transcription reaction compared to the commercial one (Figure 5a). Moreover, the pRNA scaffold seems to increase transcription efficiency only in the presence of the homemade polymerase (Figure 5b).
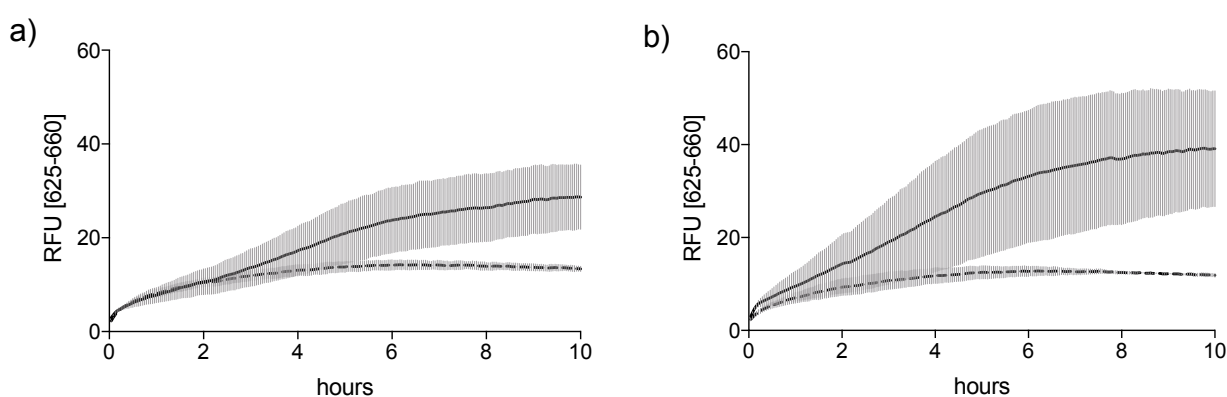
Figure 5. E. coli RNA polymerase activity test. His-tagged E. coli RNA polymerase holoenzyme function was tested by in vitro transcription of MGA (solid traces) and compared to commercial E. coli RNA polymerase (New England Biolabs) (dotted line). Plasmid templates used for the reaction were a) DC129A and b) GB008A. Both the plasmids have the E. coli constitutive promoter pTac regulating the transcription of RFP coding sequence followed by MGA coding sequence. Whereas DC129A features a simple MGA sequence, GB008A allows for the transcription of MGA as part of the pRNA scaffold which secondary structure was designed to improve aptamers folding. Reactions were run in duplicate at 37 °C and malachite green fluorescence was monitored using Rotor-Gene Q 6plex (Qiagen) (excitation: 625±5 nm; emission: 660±10 nm).

	Mass	Stock	Working conc.
E. coli RNA polymerase core enzyme	~ 390 kDa [2x α, ß, ß' and ω]	2.3 µM	126 nM
σ^{70} transcription factor	~ 70 kDa [σ]	15.6 µM	311 nM

Table 1. E. coli RNA polymerase core enzyme reconstitution. Different concentrations were tested for both the core enzyme and the transcription factor. Reported are the working concentrations used in the in vitro transcription reaction in Figure 5.

PURE factors purification

Translation factors and tRNA synthetases were purified to reconstitute the factors mix of the homemade PURE system together with the purchased enzymes responsible for ATP regeneration.

The His-tagged enzymatic components allowing for translation (listed in Table 2) *i.e.* tRNA synthetases (20 enzymes) and translation factors (10 enzymes) were over-expressed in BL21 (DE3) pLysS *E. coli* cells (Promega) and purified using benchtop Ni^{++} affinity chromatography (Figure 6).

Protein full name	Abbreviation	Plasmid	Resistance
Methionyl-tRNA formyltransferase	MTF		kan
initiation factor-1	IF1		kan
initiation factor-2	IF2		kan
initiation factor-3	IF3		kan
elongation factor thermo unstable	EF-Tu		kan
elongation factor-G	EF-G		kan
elongation factor thermo stable	EF-Ts		kan
release factor-1	RF1		kan
release factor-3	RF3		kan
ribosome recycling factor	RRF		kan
alanyl-tRNA synthetase	AlaRS (D777K)	pET28a	kan
cysteinyl-tRNA synthetase	CysRS	pET21a	amp
aspartyl-tRNA synthetase	AspRS	pET24a	kan
glutamyl-tRNA synthetase	GluRS	pET24a	kan
phenylalanyl-tRNA synthetase	PheRS	pET28a	kan
glycyl-tRNA synthetase	GlyRS	pET21a	amp
histidyl-tRNA synthetase	HisRS	pET21a	amp
isoleucyl-tRNA synthetase	IleRS	pET21a	amp
lysyl-tRNA synthetase	LysRS	pET3a	amp
leucyl-tRNA synthetase	LeuRS	pET21a	amp
methionyl-tRNA synthetase	METRS	pET24a	kan
asparaginyl-tRNA synthetase	AsnRS	pE30	amp
prolyl-tRNA synthetase	ProRS	pET21a	amp
glutaminyl-tRNA synthetase	GlnRS	pET21a	amp
arginyl-tRNA synthetase	ArgRS	pET16b	amp
seryl-tRNA synthetase	SerRS		kan
threonyl-tRNA synthetase	ThrRS	pET28a	kan
valyl-tRNA synthetase	ValRS	pET21a	amp
tyrosyl-tRNA synthetase	TyrRS	pET20	amp
triptophanyl-tRNA synthetase	TrpRS	pET21a	amp
T7 RNA polymerase	T7 RNAP	pET21a	amp

Table 2. PURE system purified protein components.
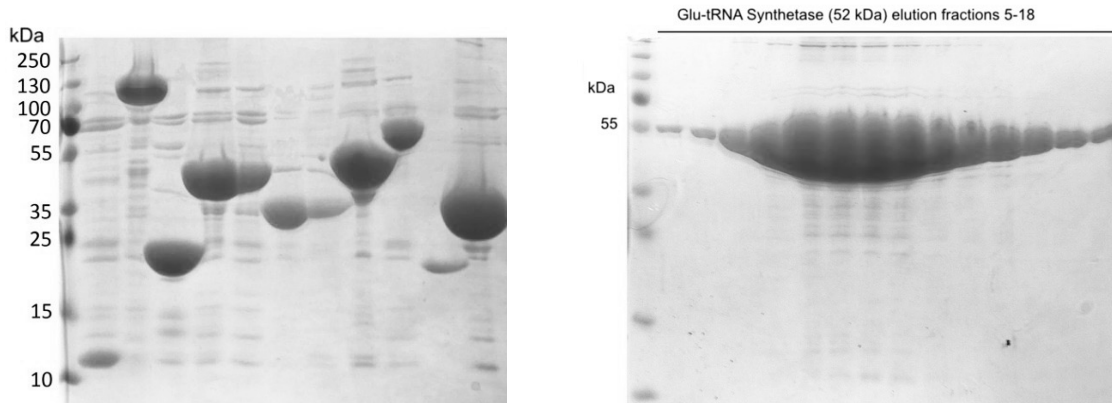
Figure 6. Purification of translation factors and tRNA synthetases. *On the left, the SDS-PAGES with samples from the translation factors purified stocks. From left to right: PageRuler Plus Protein Ladder (Thermo Fisher Scientific), IF1 (8.1 kDa), IF2 (97.3 kDa), IF3 (20.4 kDa), EF-G (77.5 kDa), EF-Tu (43.3 kDa), EF-Ts (31 kDa), EF-Ts from another purification (31 kDa), RF1 (39.6 kDa), RF3 (58.2 kDa), RRF (20.3 kDa), MTF (35 kDa). On the right, the SDS-PAGE with elution fractions samples from Glu-rRNA synthetase (52 kDa) purification.*

In most cases, the benchtop purifications of the translation yielded a good amount of protein with a good grade of homogeneity. Some proteins showed a running pattern different from the expected one. The purified tRNA synthetases not always were expressed optimally, an example is Glu-tRNA synthetase as shown in Figure 6b. In some cases, the product of more purifications had to be pooled to reach a concentrated stock.

Ribosomes were purified from the *E. coli* strain JE28. *E. coli* JE28 was genetically engineered by Sanyal and coworkers to constitutively express a His-tagged version of the L12 ribosomal protein. Four L12 proteins are part of the *E. coli* ribosome thus making JE28 a tetra-His-tagged ribosome producing strain. His-tagged ribosomes isolation was addressed with Ni^{++} affinity purification. Concentration of the ribosomes stock was assessed by absorption spectroscopy of a 100-fold diluted sample using $\varepsilon = 4.055 \times 10^{7}$ $M^{-1}cm^{-1}$ for 260 nm absorbance. Ribosomes stock normalized concentration was 4.9 μM, while A260/A280= 1.93 (1.9 is a value typical for pure ribosomes).

Church Factors purification

The six protein pools were prepared to verify the possibility to reconstitute a homemade PURE system with a significantly faster protocol. The number of purifications to be carried out using this approach are 5-fold less compared to the classical PURE system preparation[35].

Engineered *E. coli* strains purifications allowed for the preparation of 6 protein pools. Each strain was grown and the protein pools purified by benchtop Ni^{++} affinity chromatography, being all His-tagged. The protein content of each stock was verified by SDS-PAGE (Figure 7). The contents of the individual pools are reported in Table 3.
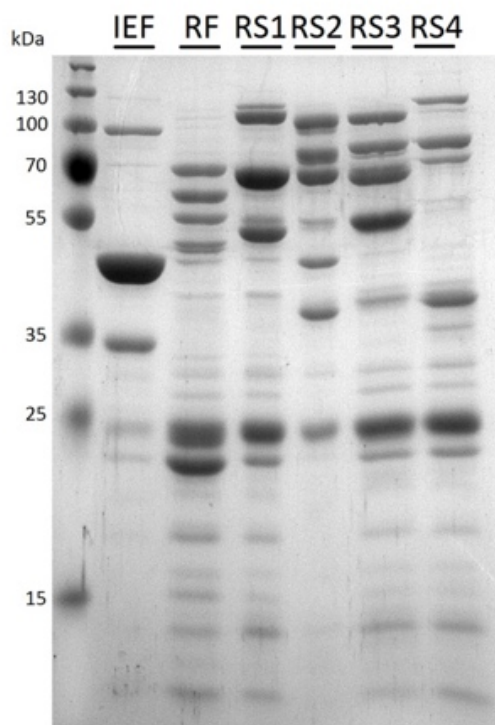
Figure 7. His-tagged PURE System factors pools purifications. Lane 1 PageRuler Plus Protein Ladder (Thermo Fisher Scientific); lane 2: IEF strain factors, lane 3: RF strain factors; lane 4: RS1 strain factors; lane 5: RS2 strain factors; lane 6: RS3 strain factors; lane 7: RS4 strain factors.

E. coli strain	His-tagged factors
IEF	EF-Ts, EF-G, EF-Tu(a), EF-Tu(b), EF4, IF1, IF2, IF3
RF	RRF, RF1, RF2, RF3
RS1	Ile-tRNA Synthetase, Pro-tRNA Synthetase, Cys-tRNA Synthetase, Leu-tRNA Synthetase, Gln-tRNA Synthetase, Ser-tRNA Synthetase
RS2	Asn-tRNA Synthetase, Tyr-tRNA Synthetase, Phe-tRNA Synthetase A, Phe-tRNA Synthetase B,Thr-tRNA Synthetase, Asp-tRNA Synthetase
RS3	Arg-tRNA Synthetase, Met-tRNA Synthetase, Glu-tRNA Synthetase, His-tRNA Synthetase, Ala-tRNA Synthetase, Lys-tRNA Synthetase
RS4	Met-tRNA Formyltransferase, Trp-tRNA Synthetase, Gly-tRNA Synthetase A, Gly-tRNA Synthetase B, Val-tRNA Synthetase

Table 3. Church strains His-tagged components. The genome of each strain was engineered by Church and colleagues in order to constitutively express a set of His-tagged components.

The purified component pools contained all the relative His-tagged proteins. A set of recurring unwanted bands can be observed among the pools, but the concentration of such protein contaminants is low and tolerable.

Homemade PURE system (Church) reaction

The homemade PURE system reaction was assembled by mixing the purified components described above with the buffer solution described above. The reaction template (DC032A) carried RFP coding sequence under T7 promoter transcription regulation. Downstream the RFP gene, the plasmid also contained the spinach aptamer[46] coding sequence. The folded spinach aptamer can bind to the small molecule (*Z*)-4-(3,5-difluoro-4-hydroxybenzylidene)-1,2-dimethyl-1H-imidazol-5(4H)-one (DFHBI). DFHBI free in solution has a very low quantum yield that strongly increases upon binding to spinach. Monitoring DFHBI fluorescence allows for the indirect quantification of the transcribed RNA levels (Figure 8).
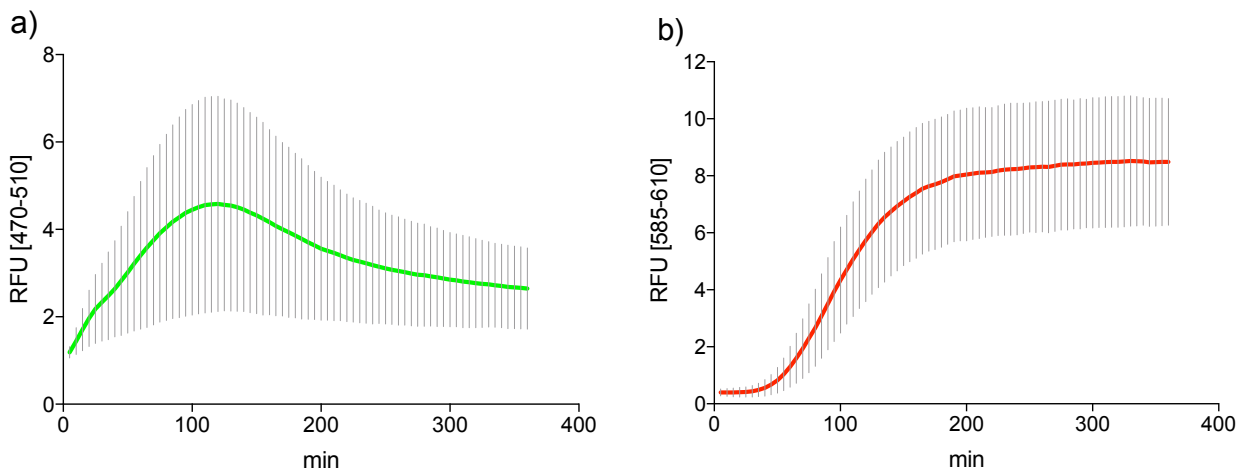
Figure 8. Homemade PURE system in vitro expression of RFP-spinach.
Homemade PURE reaction was templated with DC032A plasmid providing the coding
sequences of RFP and spinach aptamer under the transcriptional regulation of T7
*promoter. Showed are real time fluorescence data relative to **a**) RNA and **b**) protein.*
Reactions were run in duplicate at 37 °C and fluorescence was monitored using Rotor-
Gene Q 6plex (Qiagen). DFHBI fluorescence was acquired with the green channel
(excitation: 470 ± 10 nm; emission: 510 ± 5 nm). RFP fluorescence was acquired with the
orange channel (excitation: 585±5 nm; emission: 610±5nm).

The homemade PURE system works well both in transcription, monitored via spinach aptamer binding to DFHBI (Figure 8a), and translation, observed from RFP production (Figure 8b). However, even though the homemade T7 RNA polymerase was very well performing as shown above, the whole homemade PURE reaction is not as efficient as the commercial one (data not shown).

TrpR transcription regulation in the homemade PURE system (Church)

To assess whether simple transcriptional control could be reconstituted in the homemade PURE system, tryptophan repressor (TrpR) activity was tested in an *in vitro* transcription-translation reaction (Figure 9). Two different homemade PURE reactions were run using DC032A plasmid (described above) or DC076A as templates. DC076A differs from DC032A for the presence of the tryptophan operator sequence (trpO) downstream the T7 promoter controlling RFP expression. Moreover, a pT7-TrpR sequence is cloned downstream of the RFP-spinach sequence, so that TrpR is synthesized as well. The

expression of RFP-spinach should be repressed in DC076A-templated reaction as a result of TrpR binding to trpO.
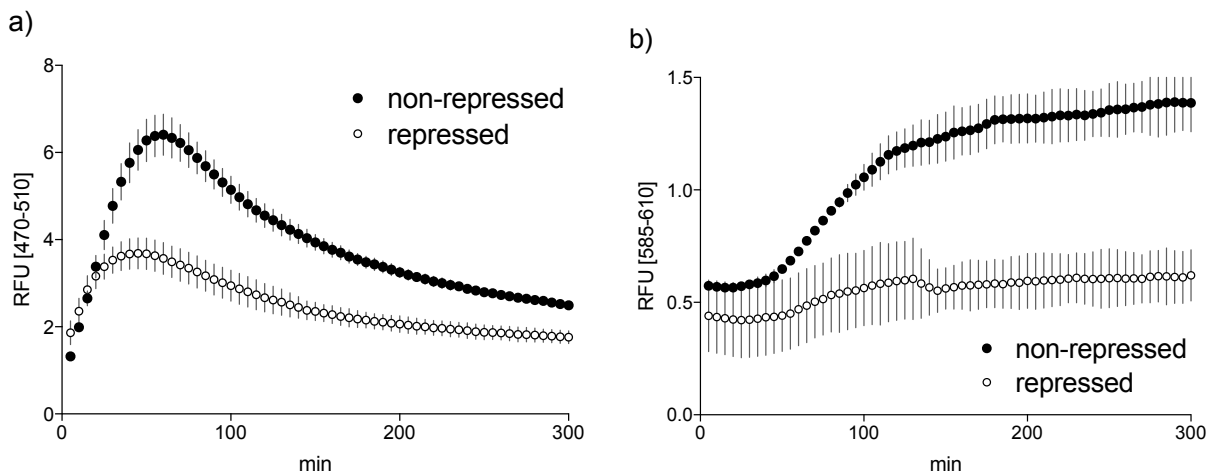
*Figure 9. TrpR transcriptional regulation of RFP expression in homemade PURE system. Homemade PURE reactions were templated by plasmid vectors DC032A (non-repressed, black circles) and DC076A (repressed, white circles). Showed are real-rime fluorescence data relative to **a**) RNA and **b**) protein. DC032A has T7 promoter driving the expression of RFP and spinach aptamer. DC076A has in addition the pT7-TrpR sequence and trpO element downstream the T7 promoter driving RFP expression. When using DC076A as template, synthesized TrpR should block transcription of RFP. Reactions were run in duplicate at 37 °C and fluorescence was monitored using Rotor-Gene Q 6plex (Qiagen). DFHBI fluorescence was acquired with the green channel (excitation: 470 ± 10 nm; emission: 510 ± 5 nm). RFP fluorescence was acquired with the orange channel (excitation: 585±5 nm; emission: 610±5nm).*

Tryptophan is already present in the PURE system reaction being one of the amino acids provided for protein synthesis. Therefore, TrpR, once synthesized, binds the available tryptophan and represses RFP-spinach transcription. Repression is not total, as shown by the RNA traces in Figure 9a, probably because some transcription of RFP-spinach was already started before trpR synthesis and activation.

S30 Crude Extract preparation and transcription-translation reaction

S30 Crude Extract yield was approximately 1 mL per liter of culture. S30 *in vitro* transcription-translation control reaction was performed using the plasmid FC045A as

template. The plasmid template carries RFP coding sequence behind the T5 promoter, recognized by endogenous *E. coli* RNA polymerase.
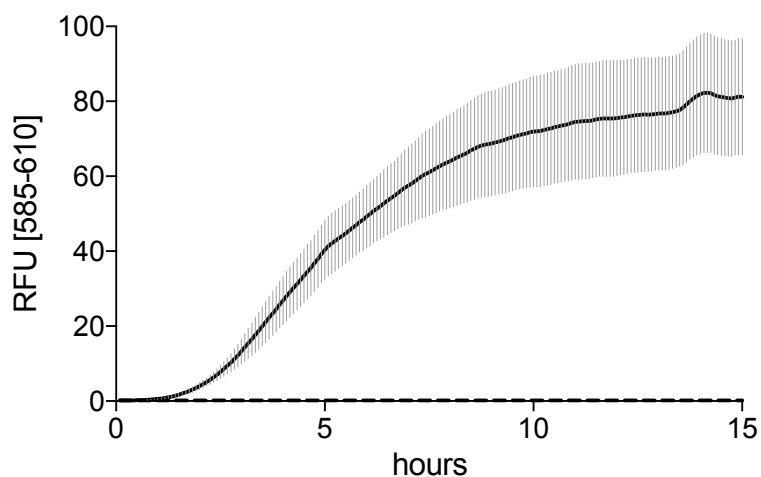
Figure 10. S30 Extract in vitro synthesis of RFP. *S30 cell-free protein expression was tested using FC045A plasmid template allowing for the E. coli RNA polymerase-dependent expression of RFP. Reactions were run in duplicate at 37 °C and fluorescence was monitored using Rotor-Gene Q 6plex (Qiagen). RFP fluorescence was acquired with the orange channel (excitation: 585±5 nm; emission: 610±5nm).*

1.3. Discussion

The aim of this study was to reconstitute an *in vitro* transcription-translation system comparable to the commercially available ones to be used for synthetic biology applications. The classic preparation of the homemade PURE led to a non-functioning system. The simplified procedure for assembling the PURE led to a poorly performing system which activity was very low when compared to the commercial kit. The S30 *E. coli* Extract is performing the best. Moreover, the procedure to prepare the S30 Crude Extract is relatively quick, robust and reproducible even if not trivial and in some parts delicate.

The PURE system was the most appealing among the different cell-free protein production platforms for many reasons. First, the PURE is by definition the most elegant synthetic biology approach to protein synthesis. Succeeding in mimicking protein synthesis with this exquisite bottom-up methodology was one of the greatest achievements in synthetic biology and molecular biology in general. Second, the commercially available PURE is very expensive. Having an unlimited resource of PURE system in the lab would change the way experiments are conceived, possibly in a more relaxed and confident manner. Last, preparing the PURE system in house could open to a lot of possibilities in terms of fine tuning or omitting virtually every component for the creation of new cell-free protein synthesis architectures. To this end, all the protein components for the reconstitution of the translation machinery were purified by means of benchtop Ni^{++} affinity chromatography exception made for creatine kinase, myokinase, nucleoside-diphosphate kinase, and pyrophosphatase. In some cases, very low purification yields were observed. Growth could be likely affected by the overexpression of enzymes with such a crucial role in *E. coli* metabolism. A tetra-His-tagged ribosome was purified as well. In the PURE system, the transcription is carried out by T7 RNA polymerase which coding sequence was cloned in an expression vector, added of the 6x Histidine tag and purified. In sight of different available choices for differential expression in the homemade PURE, also *E. coli* RNA polymerase was isolated in a combination of three chromatography purification steps: Ni^{++} affinity, heparin affinity and ion-exchange. The σ^{70} transcription factor was purified as well in two steps, by Ni^{++} affinity chromatography and ion-exchange chromatography.

The RNA polymerases were tested for transcription activity and compared to their commercial counterparts. To monitor RNA traces in real time, aptamers were used that bind fluorophores enhancing their quantum yield. T7 RNA polymerase performed better than commercial polymerase when the same amount was used for transcription, meaning that the purified stock was characterized by a higher U/µL count. *E. coli* RNA polymerase core enzyme and σ^{70} transcription factor were mixed in an *in vitro* transcription reaction to reconstitute the RNA polymerase holoenzyme. After testing different ratios between the two purified components, the optimal reaction concentrations observed were 126 nM and 311 nM for the core enzyme and the σ^{70} transcription factor, respectively. These concentrations are consistent with the fact that specific and efficient RNA synthesis from bacterial and phage promoters is achieved when the core enzyme is saturated with σ^{70} transcription factor. Purified *E. coli* RNA polymerase holoenzyme was performing better than the commercial holoenzyme. When testing *in vitro* transcription with *E. coli* RNA polymerase holoenzyme, the pRNA scaffold influence on malachite green aptamer activity was assessed. The transcription product of pRNA is reported to fold into a secondary structure that increases the stability and folding of up to three aptamers inserted into its loops. Malachite green aptamer was cloned into one of the pRNA loops and this setting was compared to the simple malachite green aptamer. Results show that pRNA is actually enhancing the folding of malachite green aptamer even if the effect is observed only when considerable amounts of RNA are produced. When the homemade PURE system was assembled, only T7 RNA polymerase transcription activity was observed. Translation of reporter fluorescent protein was not detectable. This was probably due to one or more inactive translation factor and/or tRNA synthetase.

The Church approach to PURE system allowed for a relative quick purification of the translation factors. The buffer solution was assembled and the reaction tested with a template for the expression of RFP-spinach aptamer. Finally, the homemade PURE system worked in a detectable way. A simple repression of transcription was also tested in the homemade PURE reaction to assess whether the system was performing as expected. The homemade PURE system was working but the activity was extremely low. Shown in this chapter is the highest activity reached by the homemade PURE system which is 50-fold lower than the commercial PURE.

S30 *E. coli* Crude Extract preparation needed some time to be streamlined but showed to be the best approach for achieving *in vitro* transcription-translation. After several trials, a consistent yield of 1 mL of S30 Crude Extract was obtained per liter of starting culture. Homemade S30 reaction can yield up to 150 µg/mL of RFP.

1.4. Materials and Methods

E. coli chemically competent cells preparation

This experimental procedure was adopted for every *E. coli* strain used. *E. coli* cells were scraped from glycerol stock and grown o/n at 37 °C, 220 rpm. On the next day, cells were diluted 1:100 in 50 mL of LB and incubated again at 37 °C, 220 rpm. When $OD_{600\,nm} =$ 0.5 was reached, the culture was chilled on ice for 10 min. Cells were harvested by 10 min centrifugation at 5,000 xg at 4 °C. Supernatant was discarded and the pellet re-suspended in 15 mL of Transformation buffer and incubated on ice for 15 minutes. Cells were harvested and re-suspended in 4 mL of Transformation buffer. Glycerol was added to final concentration of 20% v/v. Competent cells were aliquoted into 100 μL aliquots, flash frozen with liquid nitrogen and stored at -80 °C.

Transformation of *E. coli* chemically competent cells

This experimental procedure was adopted for every *E. coli* strain used. Chemically competent *E. coli* cells were thawed on ice and added with 10-50 ng of plasmid DNA and incubated on ice for 20 min. Heat shock was performed by incubating cells at 42 °C for 1 min. Cells were placed on ice again for 10 min. Cells were recovered by addition of 800 μL of LB and incubation at 37 °C for 45 min, 220 rpm. 50 μL from recovered culture were spread onto LB agar plates added with antibiotic.

Note: PURE system plasmids for the overexpression and purification of tRNA synthetases were provided by Professor Florian Seebeck (University of Basel)

PURE Components purification

Transformed BL21(DE3) pLysS (Promega) *E. coli* were grown o/n in LB with antibiotic starting from a single colony. The day after 1 L culture was started in LB with antibiotic by diluting the o/n culture 1:1000. When $OD_{600} = 0.6$ bacteria were induced with 1 mM

IPTG and grown for 4 additional hours. Cells were harvested by centrifugation at 5,000 x*g* at 4 °C, 20 min. Pellets were resuspended in 100 mL PURE Resuspension buffer supplemented with PMSF protease inhibitor to 1 mM final concentration. Bacteria were lysed on ice with 8 cycles of sonication 15 seconds ON / 45 seconds OFF using Analog Sonifier Cell Disruptor (Branson) output 60%. Lysate was clarified by centrifugation at 17,000 x*g* 4 °C, 30 min, twice and residual debris removed by 0.22 μm filtration.

Each purification was performed with 10 mL Ni-NTA agarose matrix (QIAGEN). Ni-NTA agarose matrix was regenerated in between each protein purification to ensure the removal of contaminants and to allow the Ni^{++} charging on nitriloacetic acid-tagged agarose beads. Regeneration was performed by washing the matrix with 5 column volumes (cv) ddH_2O, 3 cv 2% SDS, 5 cv 100% EtOH, 1 cv ddH_2O, 5 cv 0.1 M EDTA pH 8.0, 2 cv $NiSO_4$, 3 cv ddH_2O, 2 cv 6 M GuHCl 0.2 M acetic acid.

Ni-NTA agarose matrix was equilibrated with 3 cv of PURE Resuspension buffer then the cleared lysate was loaded and let pass through at 4 °C. Matrix was washed with 4 cv of PURE wash buffer. Bound His-tagged proteins were eluted with PURE elution buffer and 1.5 mL elution fractions were collected on ice. To assess which elution fractions contained the elution product 1 μL of each fraction was spotted on filter paper, stained with Staining solution for 5 min at r.t. and de-stained with flowing dH2O. Sample containing fractions were pooled, collected into 3 kDa or 10 kDa cutoff SnakeSkin™ Dialysis Tubing (Thermo Fisher Scientific) and dialyzed against 2 L PURE dialysis buffer for 2 hrs at 4 °C. Sample was dialyzed against 2 L PURE stock buffer o/n at 4 °C, split in 1 mL aliquots and stored at -80 °C.

PURE system cell-free protein synthesis

PURE system DNA plasmid templates were prepared with Plasmid Mini Kit (Qiagen). Solution A and B were prepared according to Ueda's directions[34] with the exception that T7 RNA polymerase was not added to solution B. A typical 50 μL homemade PURE system reaction was run by mixing 25 μL solution A, 5 μL solution B, 10 nM plasmid template, 60 μM DFHBI when needed, 5 μL T7 RNA polymerase, 1 μL RiboLock RNase Inhibitor (Thermo Fisher Scientific) and water. Reaction was run at 37 °C for 2-6 hours

Church Factors purification

E. coli strains genetically modified to constitutively express the His-tagged factors (strains IEF, RF, RS1, RS2, RS3 and RS4) needed to reconstitute the PURE System and His-tagged ribosomes (strain RB1), were kindly provided by Professor George Church (Harvard University). Factors and ribosomes were purified according to [35]. Each *E. coli* strain was grown in 5 mL LB with chloramphenicol at 30 °C, 220 rpm for 7 hours starting from glycerol stock. Culture was diluted 1:40 in 80 mL 2YTPG with chloramphenicol and grown for additional 14 h at 30 °C, 220 rpm. The whole 80 mL culture was used to start a 2 L 2YTPG culture with chloramphenicol and bacteria were grown at 30 °C, 220 rpm till OD_{600nm} = 3. Bacteria were harvested by centrifugation at 5,000 xg at 4 °C for 30 min.

Pellets from IEF, RF, RS1, RS2, RS3 and RS4 strains cultures were re-suspended in 200 mL Factors lysis buffer and lysed on ice with 8 cycles of sonication 15 seconds ON / 45 seconds OFF using Analog Sonifier Cell Disruptor (Branson) output 60%. Lysate was clarified by centrifugation at 4 °C, 17,000 xg, 30 min twice and by 0.22 μm filtration. Pellet from RB1 strain culture was re-suspended in 20 mL RB1 lysis buffer with 5 mL 0.1 mm glass beads (Biospec). Bacteria were lysed once by means of FastPrep-24 bead-beater (MP Biomedicals), velocity = 6.0 m/s, 30 sec. Lysate was cleared from cell debris and beads by centrifugation at 4 °C, 17,000 xg, 30 min twice and by 0.22 μm filtration. Following steps were performed using Cleared lysate was loaded on Ni-NTA matrix, previously equilibrated with 3 cv of Factors wash buffer (IEF, RF, RS1, RS2, RS3 and RS4 lysates) or RB1 wash buffer (RB1 lysate) and let pass through at 4 °C. Matrix was washed with 3 cv of Factors wash buffer or RB1 wash buffer. His-tagged factors were eluted with 3 cv of Factors elution buffer or RB1 elution buffer and 1,5 mL elution fractions were collected on ice. 1 μL from each elution fraction was spotted on filter paper and stained with Staining solution.

Sample containing fractions corresponding to IEF, RF, RS1, RS2, RS3 and RS4 purifications were pooled and dialyzed against 2 L Factors storage buffer. Molecular weight cut-off of Snakeskin Dialysis tubing (Thermo Fisher Scientific) was 3K for IEF strain and 10K for RF, RS1, RS2, RS3, RS4. Sample containing fractions corresponding to RB1 purification were pooled. Ribosomes were harvested by ultracentrifugation at 4 °C, 150,000 xg, 4 hours and resuspended in 100 µL RB1 storage buffer. Ribosomes stock concentration was determined by UV absorbance at 260 nm[47].

Church PURE system cell-free protein synthesis

DNA plasmid templates were prepared with Plasmid Mini Kit (Qiagen). Cell-free protein synthesis reaction was mixed according to Church's directions[35]. A typical Church PURE system reaction contained 700 µg/mL IEF, 370 µg/mL RF, 150 µg/mL RS, 550 µg/mL RS2, 183 µg/mL RS3, 79 µg/mL RS4, 22.3 µg/mL individual IF1, 30.9 µg/mL individual IF3, 20.0 µg/mL Arginyl-tRNA synthetase, 96.0 µg/mL Glycyl-tRNA synthetase, 0.1 mM each amino acid, 0.3 mg/mL tRNA mix, 1 mM CTP and UTP, 2.5 mM GTP, 3 mM ATP, 20 mM creatine phosphate, 10 µg/mL folinic acid, 50 mM HEPES KOH pH 7.6, 100 mM K-glutamate, 13 mM Mg-acetate, 2 mM spermidine, 2 mM DTT, 1x T7 RNA polymerase from 10x stock, 1 U/µL RiboLock RNase Inhibitor (Thermo Fisher Scientific), 10 nM DNA plasmid template, 1.5 µM His-tagged *E. coli* ribosomes or *E. coli* Ribosome (New England Biolabs), 60 µM DFHBI when needed.

Gibson Assembly

Forward and reverse primers were designed with a 20 base pairs complementarity to the sequence to be amplified. Self-dimer and hetero-dimer formation was checked online with the Oligoanalizer 3.1 (Integrated DNA Technologies). Lyophilized stocks were resuspended in DEPC water to a final concentration of 100 µM, and diluted in working 10 µM stocks. Substrates for the cloning reaction were produced by PCR-amplification with Phusion DNA polymerase (Thermo Fisher Scientific) and 5' overlapping primers with a melting temperature greater than 50 °C. 1% w/v agarose gel with 1 µL 50,000X Atlas ClearSight DNA Stain (BIOATLAS) was prepared in TAE. The electrophoretic chamber was filled with TAE. 5 µL of the PCR products were mixed with 6X DNA

Loading Dye (Thermo Fisher Scientific) to a final volume of 6 μL, and loaded on the gel. Amplicons size was assessed by running 4 μL of GeneRuler 1 kb Plus DNA Ladder (Thermo Fisher Scientific). Run was performed at a constant voltage of 120 V. The remaining volumes were incubated with 1 μL DpnI (NEB) for 1 h at 37 °C. Gibson Assembly reaction was assembled by mixing 5 μL 2X Gibson Master Mix with 75 ng vector and 3 molar equivalents of insert and ddH2O to a final volume of 10 μL. The cloning reaction was incubated for 1 h at 50 °C.

T7 RNA polymerase cloning, overexpression and purification

T7 RNA polymerase cloning and purification was performed according to [48] with modifications. T7 RNA polymerase coding sequence was amplified from pAR1219 plasmid (Sigma). pET21b was chosen as plasmid vector. Resulting construct was named GB002A. NEB Express *E. coli* cells (New England Biolabs) were transformed with GB002A, grown in 2 L LB with antibiotic till $OD_{600nm} = 0.6$, induced with 0.5 mM IPTG and grown o/n. Cells were harvested by centrifugation at 5,000 x*g* at 4 °C. Cells were resuspended in T7 resuspension buffer, lysed on ice with 8 cycles of sonication 15 seconds ON / 45 seconds OFF using Analog Sonifier Cell Disruptor (Branson) output 60%. Lysate was clarified by centrifugation at 17,000 x*g* 4 °C, 30 min, twice and residual debris removed by 0.22 μm filtration.

Ni-NTA agarose matrix was equilibrated with 3 cv of T7 Resuspension buffer then the cleared lysate was loaded and let pass through at 4 °C. Matrix was washed with 4 cv of T7 wash buffer. Bound His-tagged T7 RNA polymerase was eluted with T7 elution buffer and 1.5 mL elution fractions were collected on ice. To assess which elution fractions contained the elution product 1 μL of each fraction was spotted on filter paper, stained with Staining solution for 5 min at r.t. and de-stained with flowing dH2O. Sample containing fractions were pooled, collected 10 kDa cutoff SnakeSkin™ Dialysis Tubing (Thermo Fisher Scientific) and dialyzed against 2 L T7 stock buffer twice, for 2 hrs and o/n, at 4 °C. Sample was split in 1 mL aliquots and stored at -80 °C.

T7 RNA polymerase transcription

Transcription reaction was always added with fresh DTT to 1 mM final concentration as a significant loss in activity was observed with old T7 RNA polymerase stocks, probably due to DTT oxidation. A typical *in vitro* transcription contained 0.1 mg/mL BSA, 10 mM DTT, 35 mM $MgCl_2$, 2 mM spermidine, 2 mM ATP CTP GTP UTP, 0.1 U/mL Yeast Pyrophosphatase Inorganic (New England Biolabs), 0.4 U/µL RiboLock RNase Inhibitor (Thermo Fisher Scientific), 10 ng/µL DNA plasmid template, 200 mM HEPES, pH 7.5. *In vitro* transcription reaction was supplemented with 1 µM Malachite green when template was coding for malachite green aptamer or 60 µM DFHBI when template was coding for spinach aptamer. Fluorescence levels were monitored in real time with Rotor-Gene Q 6plex (Qiagen).

Note: pVS10 and pIA586 plasmid vectors for the overexpression and purification of E. coli RNA polymerase and σ^{70} transcription factor respectively, were kindly provided by Vladimir Svetlov (New York University School of Medicine) and Irina Artsimovitch (Ohio State University).

E. coli RNA polymerase core enzyme purification

BL21 (DE3) pLysS *E. coli* cells (Promega) transformed with pVS10 vector were incubated in 100 mL LB with ampicillin at 37 °C, 220 rpm, o/n. Culture was diluted 1:100 in 4 L LB with ampicillin, grown at 37 °C, 220 rpm till OD_{600nm} = 0.75. Bacteria were induced with 1 mM IPTG and grown for additional 3 hours at 37 °C, 220 rpm. Bacteria were harvested by centrifugation at 4 °C, 6,000 x g, 30 minutes. Pellet was re-suspended in 100 mL *E. coli* RNAP lysis buffer added with 1 mM PMSF and 1 mg/mL lysozyme and incubated for 30 min on ice. Bacteria were lysed on ice with 8 cycles of sonication 30 seconds ON / 2 min OFF using Analog Sonifier Cell Disruptor (Branson) output 60%. Lysate was clarified by centrifugation twice at 4 °C, 17,000 x*g*, 30 min.

Lysate was loaded on Ni-NTA matrix previously equilibrated with 3 cv of *E. coli* RNAP lysis buffer. Matrix was washed with 20 mL *E. coli* RNAP Ni^{++} binding buffer. Bound protein was eluted with 10 mL *E. coli* RNAP Ni^{++} elution buffer. *E. coli* RNA

polymerase containing fractions were dialyzed overnight against 2 L of *E. coli* RNAP dialysis buffer AB5.

The two following purifications were performed with Äkta FPLC (GE Healthcare). Before each purification pump was run 4 mL/min at 100% *E. coli* RNAP buffer B till conductivity stabilized around 95 mS/cm and then switched to 100% *E. coli* RNAP buffer A till conductivity stabilized around 4 mS/cm.

For heparin affinity chromatography, flow rate was set to 1 mL/min and HiPrep Heparin FF 16/10 column (GE Healthcare) was connected to the instrument and equilibrated with 5% *E. coli* RNAP buffer B till conductivity stabilized around 9.5 mS/cm. Dialyzed sample was loaded at 1 mL/min. Column was washed with 20 mL 5% B at 2 mL/min. Gradient 5% to 100% *E. coli* RNAP buffer B was applied over 200 mL at 1 mL/min. Protein elution was monitored by real time 280 nm absorbance reading. Bound protein eluted between conductivity 35 and 40 mS/cm. Fractions containing sample were pooled and dialyzed against 100 volumes of *E. coli* RNAP dialysis buffer AB5 at 4 °C, o/n.

For ion exchange chromatography, flow rate was set to 1 mL/min and Mono Q 5/50 GL column (GE Healthcare) was connected to the instrument and equilibrated with 5% *E. coli* RNAP buffer B till conductivity stabilized around 9.5 mS/cm. Column was washed with 20 mL 5% B at 2 mL/min. Gradient 5% to 100% *E. coli* RNAP buffer B was applied over 200 mL at 1 mL/min. Protein elution was monitored by real time 280 nm absorbance reading. Bound protein eluted between conductivity 20 and 30 mS/cm. Fractions containing sample were pooled and dialyzed against 500 volumes of *E. coli* RNAP dialysis buffer AB5 at 4 °C, o/n.

σ^{70} transcription factor purification

BL21(DE3) pLysS *E. coli* (Promega) transformed with pIA586 were incubated in 100 mL LB with kanamycin at 37 °C, 220 rpm, o/n. Culture was diluted 1:100 in 1 L LB + 5% v/v glucose and kanamycin and grown at 37 °C, 220 rpm till $OD_{600nm} = 0.6$. Bacteria were induced with 1 mM IPTG and grown for additional 4 hours at 30 °C, 220 rpm. Lowering the temperature is important for obtaining soluble σ^{70} protein. Bacteria were

harvested by centrifugation at 4 °C, 6,000 x g, 30 minutes. Pellet was re-suspended in 60 mL σ^{70} Ni^{++} binding buffer. Bacteria were lysed on ice with 8 cycles of sonication 30 seconds ON / 2 min OFF using Analog Sonifier Cell Disruptor (Branson), output 60%. Lysate was clarified by centrifugation twice at 4 °C, 17,000 xg, 30 min.

Lysate was passed twice through Ni-NTA matrix previously equilibrated with 3 cv of σ^{70} Ni^{++} binding buffer. Matrix was washed with 20 mL σ^{70} Ni^{++} binding buffer. Bound protein was eluted with 20 mL σ^{70} Ni^{++} elution buffer. Sample containing fractions were dialyzed overnight against 1 L of σ^{70} storage buffer at 4 °C.

For ion exchange chromatography, flow rate was set to 1 mL/min and Mono Q 5/50 GL column (GE Healthcare) was connected to the instrument and equilibrated with σ^{70} storage buffer till conductivity stabilized. Sample was loaded and column was washed with σ^{70} buffer A 2 mL/min. Gradient 0% to 100% σ^{70} buffer B was applied over 40 mL at 1 mL/min. Protein elution was monitored by real time 280 nm absorbance reading. Bound protein eluted around conductivity 40 mS/cm. Fractions containing sample were pooled, added with equal amount of 100% glycerol and stored at -80 °C.

E. coli RNA polymerase holoenzyme *in vitro* transcription reaction

E. coli RNA polymerase holoenzyme was reconstituted and tested *in vitro* by transcription of malachite green aptamer inserted or not on pRNA scaffold. A typical *E. coli* RNA polymerase *in vitro* transcription reaction contained: 1X *E. coli* RNA polymerase Reaction Buffer (New England Biolabs), 10 nM plasmid template, 0.5 mM each NTP, 120 nM *E. coli* RNA polymerase core enzyme, 300 nM σ^{70} transcription factor, 10 µM malachite green. Control reaction was performed using 0.1 U/µL *E. coli* RNA polymerase Holoenzyme (New England Biolabs) instead of the purified enzyme. Malachite green fluorescence was monitored in real time with Rotor-Gene Q 6plex (Qiagen) fluoromiter, excitation 625±5 nm emission 660±10 nm.

Note: JE28 E. coli strain expressing the His-tagged ribosome was kindly provided by professor Professor Suparna Sanyal (Uppsala University, Sweden).

His-tagged 70S ribosomes purification

Ribosomes were purified according to Sanyal directions[47]. JE28 *E. coli* cells were scraped from glycerol stock and grown o/n at 37 °C, shaking. The day after, 1 L LB culture with kanamycin was started by diluting 1:100 the o/n culture. When OD_{600} = 1.0 culture was slowly cooled down to 4 C (this step leads to the accumulation of 70s ribosomes) and bacteria harvested by centrifugation at 4,000 x*g*, 30 min. Pellet was resuspended in 200 mL 70S lysis buffer and lysed on ice with 4 cycles of sonication 5 seconds ON / 55 seconds OFF using Analog Sonifier Cell Disruptor (Branson) output 60%. Lysate was clarified by centrifugation at 4 C 17,000 x*g*, 30 min.

Ni-NTA agarose matrix was equilibrated with 3 cv of 70S lysis buffer then the cleared lysate was loaded and let pass through at 4 °C. Matrix was washed with 3 cv of 70S wash buffer. His-tagged 70S ribosomes were eluted with 3 cv of 70S elution buffer and 1,5 mL elution fractions were collected on ice. 1 µL from each elution fraction was spotted on filter paper and stained with Staining solution. Sample containing fractions were pooled and immediately dialyzed against 300 mL of 70S lysis buffer, 4 times, to remove imidazole. His-tagged 70S ribosomes were harvested by ultracentrifugation at 4 C 150,000 x*g*, 4 hrs. Pellet was re-suspended in Polymix buffer, split in aliquots, flash frozen in liquid nitrogen and stored at -80 C. Ribosomes stock concentration was assessed by absorption spectroscopy given ε = 4.055 x 10^7 $M^{-1}cm^{-1}$ for absorbance at 260 nm[47]. A260/A280 ratio was finally calculated, being 1.9 a value typical for pure ribosomes[49].

SDS-PAGE

Gels were casted under the chemical hood. Resolving gel was added with TEMED right before being poured and overlaid with 100% isopropanol. After polymerization, residual isopropanol was removed and Stacking gel was poured on top. Every well was loaded with a total of 3 µg of sample approximately. Samples were mixed with SDS-PAGE Loading buffer under chemical hood, heated at 95 °C for 5 minutes and loaded. 2.5 µL of

PageRuler Prestained Protein Ladder (Thermo Fisher Scientific) was loaded. Chamber was filled with running buffer and the run was performed at a constant voltage of 120 V. Gel was stained with staining solution for 40 min, r.t. De-staining was performed in dH_2O, shaking.

Resolving gel	X2 gels	Stacking gel	X2 gels
Resolving buffer	2.5 mL	Stacking buffer	410 µL
ddH2O	3.35 mL	ddH2O	3.8 mL
30% Acrylamide/Bis-acrylam	4 mL	30% Acrylamide/Bis-acrylamide	700 µL
10% SDS	100 µL	10% SDS	100 µL
10% APS	50 µL	10% APS	50 µL
TEMED	10 µL	TEMED	10 µL

RNA agarose gel

The electrophoretic chamber, the gel caster and the comb were cleaned with a solution of 0.1 M NaOH for 15 min, and rinsed thoroughly with distilled water. 2% w/v agarose gel was prepared in TAE buffer with 0.5 µg Ethidium bromide. 2 µL of sample and 2 µL of RNA ladder High range (Fermentas) were mixed with 2 µL of 2x RNA Loading dye (Fermentas), boiled at 70 °C and loaded on the gel. Constant voltage of 120 mA was applied for 30 min.

S30 Crude Extract preparation

E. coli Rosetta 2(DE3) strain, kindly provided by Prof. Friedrich C. Simmel, was grown in 2xYTP media supplemented with 40 mM K_2HPO_4, 22 mM KH_2PO_4, and 34 µg/mL of chloramphenicol overnight at 37 °C, 220 rpm. An aliquot was diluted to OD $_{600nm}$ = 0.01 and incubated for 3.5 h at 37 °C, 220 rpm. Cells were harvested at 6,000 x*g* for 6 min at 4 °C. Starting from the bacteria pellet, S30 Crude Extract was prepared according to Noireaux's indications[33] with the following modifications: yeast extract, tryptone, polyethylene glycol (PEG) 8000 Da, the 20 amino acids, Tris base were purchased from Sigma-Aldrich; SnakeSkinTM Dialysis Tubing was purchased from Thermo Fisher Scientific and used in place of Slide-A-Lyzer dialysis cassettes. The S30 Crude Extract final product was stored as 3-fold concentrated stock. S30 reaction energy solution and amino acid solution were prepared according to Noireaux's indications[33].

S30 *in vitro* protein synthesis reaction

S30 reaction and calibration were performed according to Noireaux's directions[33] with the following exceptions: K-glutamate was not included since no considerable advantage was observed when using it; maltose was used as supplementary energy source[50] and its working concentration was calibrated as well. A typical S30 *in vitro* transcription translation reaction contained: 1x S30 Crude Extract, 1.5 mM each amino acid, 1x energy solution, 11 mM maltose, 5 mM Mg-glutamate, 2% w/v PEG 8000, 60 µM DFHBI, 10 nM circular DNA template. 10 µL reactions were run at 37 °C and fluorescence was monitored in real time by fluorescence spectroscopy using Rotor-Gene Q 6plex (Qiagen).

Buffers table

2xYTPG	16 g/L tryptone, 10 g/L yeast extract, 5 g/L NaCl, 5 g/L glucose, 3 g/L KH_2PO_4 6.86 g/L K_2HPO_4
70S elution buffer	20 mM Tris-HCl pH 7.6, 10 mM $MgCl_2$, 150 mM KCl, 30 mM NH_4Cl, 1 mM PMSF, 0.5mg/mL Lysozyme, 10 µg/mL DNAseI, 150 mM imidazole
70S lysis buffer	20mM Tris-HCl pH 7.6, 10mM $MgCl_2$, 150mM KCl, 30mM NH_4Cl, 1 mM PMSF, 0.5mg/mL Lysozyme, 10ug/mL DNAseI
70S wash buffer	20 mM Tris-HCl pH 7.6, 10 mM $MgCl_2$, 150 mM KCl, 30 mM NH_4Cl, 1 mM PMSF, 0.5mg/mL Lysozyme, 10 µg/mL DNAseI, 5 mM imidazole
Ampicillin	100 µg/mL
Chloramphenicol	34 µg/mL
E. coli RNAP buffer A	50 mM Tris-HCl pH 6.9, 5% glycerol 0.5 mM EDTA pH 8.0, 1 mM DTT
E. coli RNAP buffer B	50 mM Tris-HCl pH 6.9 5% glycerol 0.5 mM EDTA pH 8.0, 1 mM DTT, 1.5 M NaCl
E. coli RNAP dialysis buffer AB5	50 mM Tris pH 6.9, 75 mM NaCl 5% glycerol 0.5 mM EDTA, 0.1 mM DTT
E. coli RNAP lysis buffer	50 mM Tris-HCl pH 6.9, 500 mM NaCl 5% glycerol
E. coli RNAP Ni^{++} binding buffer	50 mM Tris-HCl pH 6.9, 500 mM NaCl 5% glycerol, 20 mM Imidazole
E. coli RNAP Ni^{++} elution buffer	50 mM Tris-HCl pH 6.9, 500 mM NaCl 5% glycerol, 250 mM Imidazole
E. coli RNAP storage buffer	10 mM Tris-HCl pH 7.5, 50% glycerol, 100 mM NaCl, 0.1 mM EDTA, 0.1 mM DTT
Factors elution buffer	20 mM Tris-HOAc pH 7.6, 30 mM NH_4Cl, 150 mM KCl, 150 mM NaCl, 400 mM imidazole-HOAc, pH 7.4

Factors lysis buffer	20 mM Tris-HOAc pH 7.6, 30 mM NH_4Cl, 150 mM KCl, 150 mM NaCl, 1 mM PMSF, 6 mM β-Mercaptoethanol
Factors storage buffer	20 mM Tris-HOAc pH 7.6, 30 mM NH_4Cl, 150 mM KCl, 15 mM $Mg(OAc)_2$, 6 mM β-Mercaptoethanol, 10 µM GDP, 20% v/v Glycerol
Factors wash buffer	20 mM Tris-HOAc pH 7.6, 30 mM NH_4Cl, 150 mM KCl, 150 mM NaCl, 10 mM imidazole-HOAc (pH 7.4)
Kanamycin	50 µg/mL
LB	10 g/L tryptone, 5 g/L yeast extract, 10 g/L NaCl
Polymix Buffer	5 mM NH_4Cl, 95 mM KCl, 0.5 mM $CaCl_2$, 8 mM putrescine, 1 mM spermidine, 5 mM KH_2PO_4, 1 mM DTT
PURE dialysis buffer	50 mM Hepes-KOH, pH 7.6, 100 mM potassium chloride, 10 mM magnesium chloride, 7 mM 2-mercaptoethanol. Store at 4°C.
PURE elution buffer	50 mM Hepes-KOH, pH 7.6, 100 mM potassium chloride, 10 mM magnesium chloride, 500 mM imidazole, pH 7.6, 7 mM 2-mercaptoethanol
PURE Resuspension buffer	50 mM Hepes-KOH, pH 7.6, 1 M ammonium chloride, 10 mM magnesium chloride, 7 mM 2-mercaptoethanol, 1 mM PMSF.
PURE stock buffer	50 mM Hepes-KOH, pH 7.6, 100 mM potassium chloride, 10 mM magnesium chloride, 30% glycerol,7 mM 2-mercaptoethanol. Store at 4°C.
PURE wash buffer	50 mM Hepes-KOH, pH 7.6, 100 mM potassium chloride, 10 mM magnesium chloride, 20 mM imidazole, pH 7.6, 7 mM 2-mercaptoethanol.
RB1 elution buffer	10 mM Tris-HOAc pH 7.6, 60 mM NH_4Cl, 15 mM $MgCl_2$, 0.5 mM EDTA, 150 mM imidazole
RB1 lysis buffer	10 mM Tris-HOAc pH 7.6, 60 mM NH_4Cl, 15 mM $MgCl_2$, 0.5 mM EDTA, 1 mM PMSF protease inhibitor
RB1 storage buffer	20 mM Tris-HOAc pH 7.6, 30 mM NH_4Cl, 15 mM $MgCl_2$, 150 mM KCl
RB1 wash buffer	10 mM Tris-HOAc pH 7.6, 60 mM NH_4Cl, 15 mM $MgCl_2$, 0.5 mM EDTA, 5 mM imidazole
Resolving buffer	1.5 M Tris-HCl, pH 8.8
SDS-PAGE Loading buffer (3X)	240 mM Tris-HCl, pH 6.8, 6% w/v SDS, 30% v/v glycerol, 15% v/v β-mercaptoethanol, 0.06% w/v Bromophenol Blue
Stacking buffer	1 M Tris-HCl, pH 6.8
Staining solution	1% w/v Coomassie Brilliant Blue, 40% v/v methanol, 10% v/v acetic acid
T7 elution buffer	50 mM sodium phosphate, pH 8.0, 300 mM NaCl, 10% glycerol, 0.5 mM DTT 500mM Imidazole
T7 resuspension buffer	50 mM sodium phosphate pH 8.0, 300 mM NaCl, 0.5 mM DTT 1mM PMFS (Proteinase inhibitor)

T7 stock buffer	50 mM Tris-HCl pH 7.9, 100 mM NaCl, 1 mM DTT, 0.1 mM EDTA, 0.1% Triton X-100, 50% Glycerol
T7 wash buffer	50 mM sodium phosphate, pH 8.0, 300 mM NaCl, 10% glycerol, 0.5 mM DTT, 20 mM imidazole
TAE buffer	40 mM Tris-HCl, 1 mM EDTA pH 8.0, 0.1% v/v acetic acid
Transformation buffer	10 mM Tris-HCl, pH 7.0, 50 mM $CaCl_2$
σ^{70} buffer A	50 mM Tris-HCl pH 8.0, 10% v/v glycerol, 0.1 mM EDTA, 0.1 mM DTT, 0.1 M NaCl
σ^{70} buffer B	50 mM Tris-HCl pH 8.0, 10% v/v glycerol, 0.1 mM EDTA, 0.1 mM DTT, 0.5 M NaCl
σ^{70} Ni^{++} binding buffer	20 mM Tris-HCl, pH 8.0, 5 mM Imidazole, 500 mM NaCl,1 mM PMSF
σ^{70} Ni^{++} elution buffer	20 mM Tris-HCl, pH 8.0, 50 mM Imidazole, 500 mM NaCl,1 mM PMSF
σ^{70} storage buffer	50 mM Tris-HCl pH 8.0, 10% v/v glycerol, 0.1 mM EDTA, 0.1 mM DTT

1.5. References

1. Zamecnik, P. C. & Frantz, I. D. Incorporation in vitro of radioactive carbon from carboxyl-labeled dl-alanine and glycine into proteins of normal and malignant rat livers. *J. Biol. Chem.* **175,** 299–314 (1948).

2. Mao, Y., Liu, H., Liu, Y. & Tao, S. Deciphering the rules by which dynamics of mRNA secondary structure affect translation efficiency in Saccharomyces cerevisiae. *Nucleic Acids Res.* **42,** 4813–22 (2014).

3. Lamborg, M. R. & Zamecnik, P. C. Amino acid incorporation into protein by extracts of E. coli. *Biochim. Biophys. Acta* **42,** 206–211 (1960).

4. Bank, A. & Marks, P. A. Protein synthesis in a cell free human reticulocyte system: ribosome function in thalassemia. *J. Clin. Invest.* **45,** 330–336 (1966).

5. Schweet, R., Lamfrom, H. & Allen, E. THE SYNTHESIS OF HEMOGLOBIN IN A CELL-FREE SYSTEM. *Proc. Natl. Acad. Sci. U. S. A.* **44,** 1029–35 (1958).

6. Littlefield, J. W., Keller, E. B., Gross, J. & Zamecnik, P. C. Studies on cytoplasmic ribonucleoprotein particles from the liver of the rat. *J. Biol. Chem.* **217,** 111–23 (1955).

7. Hoagland, M. B., Keller, E. B. & Zamecnik, P. C. Enzymatic carboxyl activation of amino acids. *J. Biol. Chem.* **218,** 345–58 (1956).

8. Smith, H. O. & Welcox, K. W. A Restriction enzyme from Hemophilus influenzae. *J. Mol. Biol.* **51,** 379–391 (1970).

9. Mandel, M. & Higa, A. Calcium-dependent bacteriophage DNA infection. *J. Mol. Biol.* **53,** 159–62 (1970).

10. Nirenberg, M. W. & Matthaei, J. H. The dependence of cell-free protein synthesis in E. coli upon naturally occurring or synthetic polyribonucleotides. *Proc. Natl. Acad. Sci. U. S. A.* **47,** 1588–602 (1961).

11. Yin, G. *et al.* Aglycosylated antibodies and antibody fragments produced in a scalable in vitro transcription-translation system. *MAbs* **4,** 217–225 (2012).

12. Ryabova, L. A., Desplancq, D., Spirin, A. S. & Plückthun, A. Functional antibody production using cell-free translation: Effects of protein disulfide isomerase and chaperones. *Nat. Biotechnol.* **15,** 79–84 (1997).

13. Salehi, A. S. M. *et al.* Cell-free protein synthesis of a cytotoxic cancer therapeutic: Onconase production and a just-add-water cell-free system. *Biotechnol. J.* **11,** 274–281 (2016).

14. Martemyanov, K. A., Shirokov, V. A., Kurnasov, O. V., Gudkov, A. T. & Spirin, A. S. Cell-Free Production of Biologically Active Polypeptides: Application to the Synthesis of Antibacterial Peptide Cecropin. *Protein Expr. Purif.* **21,** 456–461 (2001).

15. Zubay, G. In Vitro Synthesis of Protein in Microbial Systems. *Annu. Rev. Genet.* **7,** 267–287 (1973).

16. Nevin, D. E. & Pratt, J. M. A coupled in vitro transcription-translation system for the exclusive synthesis of polypeptides expressed from the T7 promoter. *FEBS Lett.* **291,** 259–263 (1991).

17. Craig, D., Howell, M. T., Gibbs, C. L., Hunt, T. & Jackson, R. J. Plasmid cdna-directed protein synthesis in a coupled eukaryotic in vitro transcription-translation system. *Nucleic Acids Res.* **20,** 4987–4995 (1992).

18. Campbell, E. A. *et al.* Structural mechanism for rifampicin inhibition of bacterial RNA polymerase. *Cell* **104,** 901–912 (2001).

19. Tabor, S. Expression Using the T7 RNA Polymerase/Promoter System. in *Current Protocols in Molecular Biology* (2001). doi:10.1002/0471142727.mb1602s11

20. Shimizu, Y. *et al.* Cell-free translation reconstituted with purified components. *Nat. Biotechnol.* **19,** 751–755 (2001).

21. Shimizu, Y., Kuruma, Y., Ying, B.-W., Umekage, S. & Ueda, T. Cell-free translation systems for protein engineering. *FEBS J.* **273,** 4133–4140 (2006).

22. Forster, A. C., Cornish, V. W. & Blacklow, S. C. Pure translation display. *Anal. Biochem.* **333,** 358–364 (2004).

23. Ohashi, H., Shimizu, Y., Ying, B. W. & Ueda, T. Efficient protein selection based on ribosome display system with purified components. *Biochem. Biophys. Res. Commun.* **352,** 270–276 (2007).

24. Villemagne, D., Jackson, R. & Douthwaite, J. A. Highly efficient ribosome display selection by use of purified components for in vitro translation. *J. Immunol. Methods* **313,** 140–148 (2006).

25. PURExpress® Disulfide Bond Enhancer | NEB. Available at: https://www.neb.com/products/e6820-purexpress-disulfide-bond-enhancer#FAQs & Tech Tips. (Accessed: 29th January 2018)

26. Kuruma, Y., Nishiyama, K. I., Shimizu, Y., Müller, M. & Ueda, T. Development of a minimal cell-free translation system for the synthesis of presecretory and integral membrane proteins. *Biotechnol. Prog.* **21,** 1243–1251 (2005).

27. Hong, S. H., Kwon, Y.-C. & Jewett, M. C. Non-standard amino acid incorporation into proteins using Escherichia coli cell-free protein synthesis. *Front. Chem.* **2,** (2014).

28. Köhrer, C. & Rajbhandary, U. L. Proteins with One or More Unnatural Amino Acids. in *The Aminoacyl-tRNA Synthetases* 1–11 (2005).

29. Hirao, I., Kanamori, T. & Ueda, T. Cell-Free Synthesis of Proteins with Unnatural Amino Acids. The PURE System and Expansion of the Genetic Code. in *Protein Engineering* 271–290 (2009). doi:10.1007/978-3-540-70941-1_10

30. Niwa, T. *et al.* Bimodal protein solubility distribution revealed by an aggregation analysis of the entire ensemble of Escherichia coli proteins. *Proc. Natl. Acad. Sci.* **106,** 4201–4206 (2009).

31. Niwa, T., Kanamori, T., Ueda, T. & Taguchi, H. Global analysis of chaperone effects using a reconstituted cell-free translation system. *Proc. Natl. Acad. Sci.* **109,** 8937–8942 (2012).

32. Hillebrecht, J. R. & Chong, S. A comparative study of protein synthesis in in vitro systems: from the prokaryotic reconstituted to the eukaryotic extract-based. *BMC Biotechnol* **8,** 58 (2008).

33. Sun, Z. Z. *et al.* Protocols for implementing an Escherichia coli based TX-TL cell-free expression system for synthetic biology. *J. Vis. Exp.* e50762 (2013). doi:10.3791/50762

34. Shimizu, Y. & Ueda, T. PURE technology. *Methods Mol. Biol.* **607,** 11–21 (2010).

35. Wang, H. H. *et al.* Multiplexed in vivo his-tagging of enzyme pathways for in vitro single-pot multienzyme catalysis. *ACS Synth. Biol.* **1,** 43–52 (2012).

36. Gil, R., Silva, F. J., Pereto, J. & Moya, A. Determination of the Core of a Minimal Bacterial Gene Set. *Microbiol. Mol. Biol. Rev.* **68,** 518–537 (2004).

37. de Souza, T. P., Stano, P. & Luisi, P. L. The minimal size of liposome-based model cells brings about a remarkably enhanced entrapment and protein synthesis. *ChemBioChem* **10,** 1056–1063 (2009).

38. Noireaux, V. & Libchaber, A. A vesicle bioreactor as a step toward an artificial cell assembly. *Proc. Natl. Acad. Sci.* **101,** 17669–17674 (2004).

39. Courtois, F. *et al.* An integrated device for monitoring time-dependent in vitro expression from single genes in picolitre droplets. *ChemBioChem* **9,** 439–446 (2008).

40. Lentini, R. *et al.* Two-Way Chemical Communication between Artificial and Natural Cells. *ACS Cent. Sci.* **3,** 117–123 (2017).

41. Rampioni, G. *et al.* Synthetic cells produce a quorum sensing chemical signal perceived by *Pseudomonas aeruginosa*. *Chem. Commun.* (2018). doi:10.1039/C7CC09678J

42. Jewett, M. C. & Forster, A. C. Update on designing and building minimal cells. *Current Opinion in Biotechnology* **21,** 697–703 (2010).

43. Forster, A. C. & Church, G. M. Towards synthesis of a minimal cell. *Molecular Systems Biology* **2,** (2006).

44. Mavelli, F. & Stano, P. Experiments on and Numerical Modeling of the Capture and Concentration of Transcription-Translation Machinery inside Vesicles. *Artif. Life* **21,** 445–463 (2015).

45. Garamella, J., Marshall, R., Rustad, M. & Noireaux, V. The All *E. coli* TX-TL Toolbox 2.0: A Platform for Cell-

Free Synthetic Biology. *ACS Synth. Biol.* **5,** 344–355 (2016).

46.   Kolpashchikov, D. M. Binary Malachite Green Aptamer for Fluorescent Detection of Nucleic Acids. (2005). doi:10.1021/JA0529788

47.   Shu, D., Khisamutdinov, E. F., Zhang, L. & Guo, P. Programmable folding of fusion RNA in vivo and in vitro driven by pRNA 3WJ motif of phi29 DNA packaging motor. *Nucleic Acids Res.* **42,** e10 (2014).

48.   Paige, J. S., Wu, K. Y. & Jaffrey, S. R. RNA mimics of green fluorescent protein. *Science (80-.).* **333,** 642–646 (2011).

49.   Ederth, J., Mandava, C. S., Dasgupta, S. & Sanyal, S. A single-step method for purification of active His-tagged ribosomes from a genetically engineered Escherichia coli. *Nucleic Acids Res.* **37,** (2009).

50.   Ellinger, T. & Ehricht, R. Single-step purification of T7 RNA polymerase with a 6-histidine tag. *Biotechniques* **24,** 718–720 (1998).

51.   Spedding, G. (Gary). *Ribosomes and protein synthesis : a practical approach*. (IRL Press at Oxford University Press, 1990).

52.   Fujiwara, K. & Doi, N. Biochemical Preparation of Cell Extract for Cell-Free Protein Synthesis without Physical Disruption. *PLoS One* **11,** e0154614 (2016).

Chapter 2.

Cell-free transcription is more variable than translation

2.1. Introduction

Regardless of the final application of synthetic biology, from investigating how life works to the development of new technologies, the exploited tools must be characterized by simple but stringent qualities. First, the tools must feature well known and characterized mechanisms. Second, the tools must allow for a predictable use in order to grant strongly reproducible output and results. Most of the tools used in synthetic biology fulfill these requirements[1], although when it comes to cell-free expression systems and related applications, complexity increases and even a reproducible outcome cannot easily be predicted beforehand. This leads to the conclusion that the knowledge of protein expression *in vivo* can be transposed to *in vitro* systems only to certain extent. It becomes also clear that, even if we are dealing with one of the basic components of bottom-up synthetic biology, a comprehensive characterization of cell-free expression is needed.

The relationship between the kinetics of mRNA folding and gene expression involve many factors and are still not sufficiently understood[2]. Most likely this is due to the fact that the dynamics ruling the folding of mRNA can lead to very complex architectures, considering that some RNA molecules can even fold up into protein-like structures with catalytic activity[3].

This leads to the consideration that a deeper understanding of the role that RNA folding plays in the translation process is needed. Despite not shedding light on the pure mechanisms of this proposed phenomenon, the work presented in this chapter is an attempt to provide stronger evidences that *in vitro* translation is more variable than transcription and that this is at least partially due to *a*) the higher system complexity of translation compared to transcription and *b*) the GC content and secondary structures of mRNA.

2.2. Results

Variability of RNA and protein levels in an *E. coli* cell-free extract

In our laboratory, it was shown by Fabio Chizzolini that the variability in *in vitro* protein translation is greater than the variability in mRNA transcription[4]. In particular, he expressed BFP and RFP with the PURE System behind four different T7 transcriptional promoters and four different ribosome binding sites, for a total of 16 combinations with predictable RNA and protein outputs. He observed that the relative transcriptional promoter strength gave predictable distributions of mRNA concentrations regardless of the strength of the RBS. Instead, when using different RBS sequences, the concentration of protein showed a poor correlation between constructs encoding RFP and BFP, for all four transcriptional promoters. Low coefficients of variation in mRNA levels for both genetic constructs were consistent with the fact that transcription with the PURE System relies on a single enzyme, T7 RNA Polymerase. On the other hand, the large number of proteins required to synthesize proteins could explain the higher coefficients of variation observed for translation of RFP and BFP. Moreover, the DNA template for mRNA transcription comes as a concentration-defined double stranded molecule usually characterized by a consistent structure regardless of sequence. Conversely, the mRNA template for protein production folds in a sequence-dependent manner into complex secondary and tertiary structures which would be expected to affect the efficiency of translation, as observed.

To determine whether the increased variability in translation was dependent on the RNA polymerase or simply the result of some features of the PURE system, the measurement was repeated with both T7 and *E. coli* transcriptional promoters and their corresponding RNA polymerase to drive the expression of RFP using an *E. coli*-based cell extract. mRNA levels were measured based on the fluorescence of the Spinach aptamer encoded downstream of the RFP in the presence of the DFHBI ligand (Figure 1).
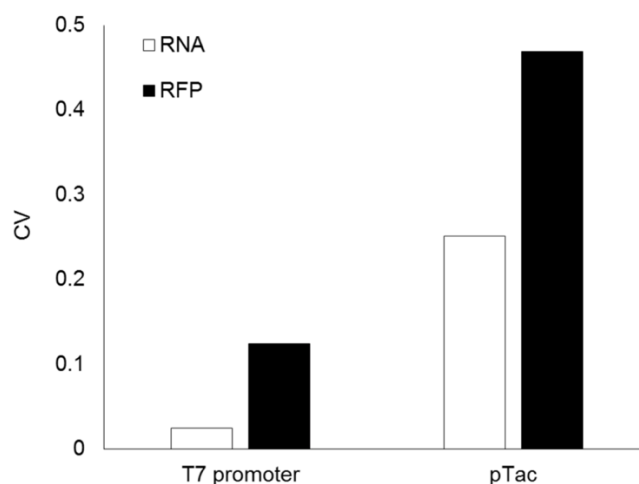
Figure 1. Variability of RNA and protein levels in an E. coli cell-free extract.
Plotted data represent the coefficient of variation of RNA and RFP (white and black bars
respectively) for both T7 and pTac promoters for reactions run on the same day with the
same batch of cell extract. The coefficient of variation was calculated for transcription
after 1 h (the point of maximal RNA) and for translation after 6 h. The coefficient of
variation was calculated over relative fluorescence intensities[4].

The calculated coefficient of variation was 5-fold larger for translation than for transcription using T7 RNA polymerase and 1.9-fold larger with *E. coli* RNA polymerase (Figure 1). The coefficient of variation was 10.4-fold higher for transcription with *E. coli* RNA Polymerase than with T7 RNA Polymerase, consistent with the multi-subunits structure of the *E. coli* RNA Polymerase holoenzyme.

Influence of RNA folding on transcription-translation

The evidences that when dealing with *in vitro* transcription-translation, even of a single gene, the RBS sequence does not allow for predictable and consistent protein output, reflects a dependence on the entire sequence of the mRNA. In fact, different RNA sequences have the ability to fold differently. Different RNA secondary structures will be characterized by diverse complexities and stabilities, which will affect accessibility of the RBS sequence as well as the initiation of translation[5], and thus ribosome density[6].

To further investigate whether RNA folding impacted the cell-free expression of protein, four different genetic sequences encoding BFP were tested. The original BFP

sequence, codon optimized for yeast and bacteria, was re-synthesized to maintain the same amino acid sequence but to have maximal or minimal GC content, and an additional sequence codon optimized construct for expression in *E. coli* was synthesized. PURE system templates were then generated by PCR amplification of the BFP coding sequences using primers to introduce the same T7 promoter upstream of the RBS. mRNA measurements were based on the fluorescence of the Spinach aptamer coded downstream of the BFP. Resulting RNA and BFP protein yields are shown in Figure 2.
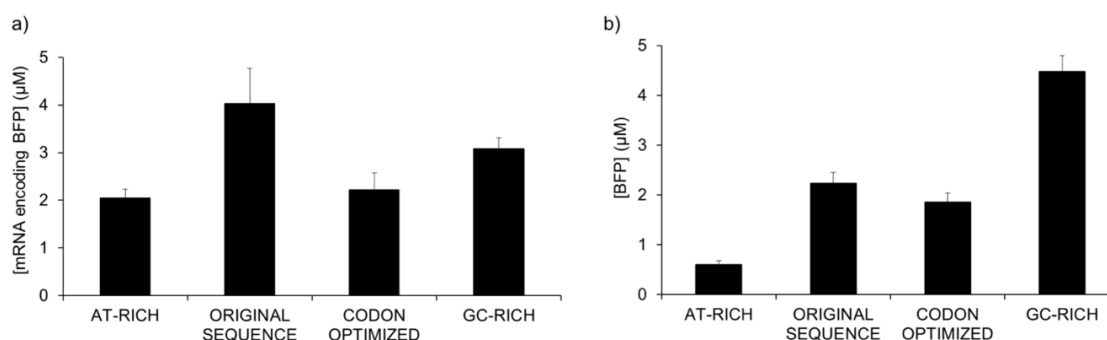

Figure 2. Different GC contents of BFP coding sequence lead to differences in translation but not transcription. Variants of the blue fluorescent protein Azurite were generated with different percentages of GC content in order to probe the relationship between mRNA structure and protein expression in PURE system reactions. PURE system reactions were incubated for 6 hours at 37 °C with the different templates for the production of different coding sequences. Both transcription and translation were monitored using fluorescence. Samples tested were, from lower GC content to higher GC content, the following: NG046 (AT rich) (GC content: 30.4%), NG045 (original sequence) (GC content: 36.27%), NG047 (codon optimized sequence) (GC content: 47.14%), NG048 (GC rich) (GC content: 59.97%)[4].

The GC content appeared to impact the amount of synthesized protein (Figure 2b). Conversely, the concentration of mRNA seemed not to be affected in a clear manner (Figure 2a). In order to focus on the effect on translation, the protein concentration was divided by the mRNA concentration (Figure 3).
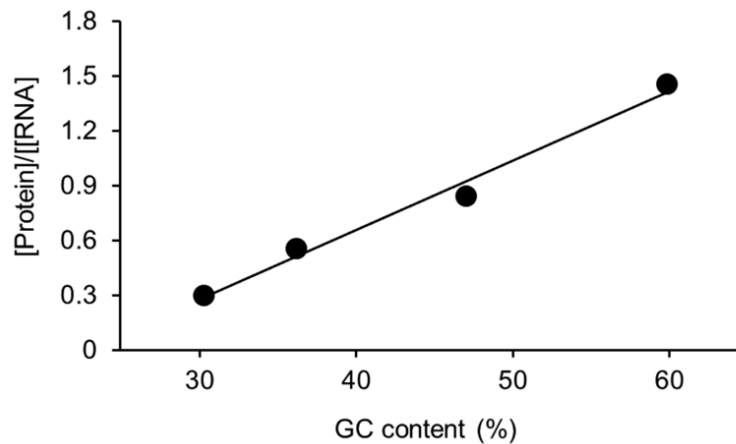
Figure 3. GC content of the coding sequence of BFP affects the synthesis of protein. The coding sequence of the protein was modified to maximize either the AT or GC content. Additionally, a codon-optimized version of the coding sequence was generated to assess the impact on translation. Each construct was expressed with the PURE system. The DNA constructs from lower GC content to higher GC content were NG046 (AT-rich, GC content: 30.4%), NG045 (original sequence, GC content: 36.3%), NG047 (codon-optimized, GC content: 47.1%), and NG048 (GC-rich, GC content: 60.0%). $R^2 = 0.985$. Adapted from Chizzolini et al. [4]

Protein over RNA ratios revealed a positive correlation between GC content and protein expression. Although the mechanism underlying this effect is yet to be elucidated, similar data were previously observed *in vivo* in *Saccharomyces cerevisiae* where genes with high protein abundance showed more stable folds of mRNA. Furthermore, folding strength was also observed to strongly correlate with ribosomal density on mRNA[7].

2.3. Discussion

Although more work is needed to determine how robust the relationship between GC content and protein expression is with bacterial systems, it does appear that mRNA folding significantly affects the expression of protein *in vitro*. Previous *in vivo* studies on the initiation of translation show that high protein expression may be best achieved with sequences characterized by low structure spanning from the RBS region[8] to the first 13 nucleotides of the coding sequence[5]. Together with data shown here, these findings suggest that the strongest translation output comes with low RBS sequences and high GC content across the gene.

To deepen the knowledge of the influence of RNA folding on protein synthesis, further steps should be taken. The approach of monitoring translation outputs using sequences with different GC content may be repeated with other reporters both with the PURE system and bacterial extract. Extracts contain possibly all the soluble proteins and enzymes found in the host they are based on. That is, the S30 *E. coli*-based extract could arguably preserve protein factors other than the minimal set required for polypeptide synthesis. Comparison of the two *in vitro* transcription systems could provide insights on the influence on translation efficiency of different proteins that bind both the RNA and the ribosome[9], certainly not present in a defined system such as the PURE system. *In vitro* protein synthesis systems can also be templated with previously transcribed mRNA molecules resulting in un-coupled gene expression. Un-coupled gene expression has been shown to strongly reduce protein synthesis efficiency due to mRNA folding in absence of ribosomes[10]. According to the findings presented here, a partial recovery of efficiency in un-coupled gene expression should be observed by using mRNA templates with lower GC content and synonymous encoded information. The simplest approach to start with, may be to identify a limited set of candidate sequences for laboratory screening, exploiting informatics prediction tools involving RNA folding and gene expression variability[11].

2.4. Materials and methods

S30 Extract cell-free transcription-translation

E. coli-based S30 Crude Extract was prepared as described in Chapter 1, Materials and Methods section. A typical S30 *in vitro* transcription translation reaction contained: 1x S30 Crude Extract, 1.5 mM each amino acid, 1x energy solution, 11 mM maltose, 5 mM Mg-glutamate, 2% (w/v) polyethylene glycol (PEG) 8000, 60 µM (Z)-4-(3,5-difluoro-4-hydroxybenzylidene)-1,2-dimethyl-1H-imidazol-5(4H)-one (DFHBI) (Lucerna), 10 nM circular DNA template. 10 µL reactions were assembled on ice and run at 30 °C. Fluorescence was monitored in real time using a Rotor-Gene Q 6plex (Qiagen). The green channel was used to detect Spinach (excitation: 470 ± 10 nm; emission: 510 ± 5 nm), and the orange channel was used to detect RFP (excitation: 585 ± 5 nm; emission: 610 ± 5 nm).

PURE System cell-free transcription-translation

Transcription-translation reactions (9 µL) with the PURExpress in vitro protein synthesis kit (New England Biolabs) contained 12.6 nM of linear DNA template and 4 units of human placenta RNase inhibitor (New England BioLabs). When needed, DFHBI was added to a final concentration of 60 µM. The reaction components were assembled on ice and the reaction was initiated by incubation at 37 °C. Reactions were monitored for 6 h with a Rotor-Gene Q 6plex system (Qiagen). The green channel was used to detect Spinach (excitation: 470 ± 10 nm; emission: 510 ± 5 nm), and the blue channel was used to detect BFP (excitation: 365 ± 20 nm; emission: 460 ± 20 nm).

Protein and RNA Standard Curves

Standard curves to translate protein fluorescence intensity into molar concentrations were generated by using over-expressed and purified recombinant His-tagged Azurite (BFP). Each His-tagged construct was purified as described previously[12]. Analogous standard curve for RNA was generated using purified RNA. The sequence encompassing transcriptional promoter, RBS, BFP coding sequence, and the Spinach aptamer was

amplified by PCR. The amplification product was run on a 1% (w/v) agarose gel, extracted and purified using Wizard Plus SV PCR cleanup system (Promega), and used as template for *in vitro* transcription reaction. RNA was synthesized in a 750 µL *in vitro* transcription reaction as described in Chapter 1, Materials and Methods section using 7.5 µL of purified His-tagged T7 RNA Polymerase and 30 nM of purified PCR product as template. Transcribed RNA was purified using E.Z.N.A. MicroElute RNA Clean Up Kit (Omega Bio-tek). Different sample dilutions were loaded on a 2% (w/v) agarose gel and bands intensities compared to RiboRuler High Range RNA Ladder (Thermo Scientific) for quantification with ImageJ[13]. Different concentrations of transcribed RNA were incubated with 60 µM DHFBI to plot a standard curve for fluorescence to concentration conversion.

2.5. References

1.   MacDonald, I. C. Tools and applications in synthetic biology. *Adv. Drug Deliv. Rev.* **105,** 20–34 (2016).

2.   Espah Borujeni, A., Channarasappa, A. S. & Salis, H. M. Translation rate is controlled by coupled trade-offs between site accessibility, selective RNA unfolding and sliding at upstream standby sites. *Nucleic Acids Res.* **42,** 2646–2659 (2014).

3.   Doherty, E. A. & Doudna, J. A. Ribozyme Structures and Mechanisms. *Annu. Rev. Biochem.* **69,** 597–615 (2000).

4.   Chizzolini, F. *et al.* Cell-Free Translation Is More Variable than Transcription. *ACS Synth. Biol.* **6,** 638–647 (2017).

5.   Espah Borujeni, A. *et al.* Precise quantification of translation inhibition by mRNA structures that overlap with the ribosomal footprint in N-terminal coding sequences. *Nucleic Acids Res.* **45,** 5437–5448 (2017).

6.   Mao, Y., Liu, H., Liu, Y. & Tao, S. Deciphering the rules by which dynamics of mRNA secondary structure affect translation efficiency in Saccharomyces cerevisiae. *Nucleic Acids Res.* **42,** 4813–22 (2014).

7.   Zur, H. & Tuller, T. Strong association between mRNA folding strength and protein abundance in S. cerevisiae. *EMBO Rep.* **13,** 272–7 (2012).

8.   Kudla, G., Murray, A. W., Tollervey, D. & Plotkin, J. B. Coding-Sequence Determinants of Gene Expression in Escherichia coli. *Science (80-.).* **324,** 255–258 (2009).

9.   Babitzke, P., Baker, C. S. & Romeo, T. Regulation of translation initiation by RNA binding proteins. *Annu. Rev. Microbiol.* **63,** 27–44 (2009).

10.   Hansen, M. M. K. *et al.* Protein Synthesis in Coupled and Uncoupled Cell-Free Prokaryotic Gene Expression Systems. *ACS Synth. Biol.* **5,** 1433–1440 (2016).

11.   Salis, H. M. The Ribosome Binding Site Calculator. in *Methods in enzymology* **498,** 19–42 (2011).

12.   Chizzolini, F., Forlin, M., Cecchi, D. & Mansy, S. S. Gene Position More Strongly Influences Cell-Free Protein Expression from Operons than T7 Transcriptional Promoter Strength. *ACS Synth. Biol.* **3,** 363–371 (2014).

13.   Schneider, C. A., Rasband, W. S. & Eliceiri, K. W. NIH Image to ImageJ: 25 years of image analysis. *Nat. Methods* **9,** 671–675 (2012).

Chapter 3.

Towards artificial cells networks

3.1. Introduction

Note: the artificial cells network project and the mentioned experiment are credited to Dario Cecchi.

In synthetic biology, a considerable defect of artificial cells (bottom-up approach) is the lack of a mechanisms for self-sustainment that is instead present in engineered living cells (top-down approach). Besides few strategies aimed at the restoration of energy in cell-free transcription-translation reactions[1,2], artificial cells are not yet able to efficiently use the available resources in their environment. To overcome this issue, the establishment of a proof-of-concept artificial cells network is proposed for the accomplishment of a major task in a cascade-like signal transduction. To this end, the possibility to set communication pathways between different kinds of artificial cells was envisioned. Not only lipid vesicles but also other kinds of artificial cells are involved in the network. A type of artificial cells used in this network collaboration are proteinsomes. These structures based on protein-polymer conjugates constitute a semi-permeable membrane, which pore size can vary according to the modified protein used and to all those conditions affecting protein folding, such as temperature, pH and ionic strength. Enzymes can perform catalytic reactions both on the membrane and in the lumen of these compartments[3]. Simple cargo liposomes and natural engineered cells are also present in the network design.

The network cascade starts with lipid-based artificial cells encapsulating a transcription-translation machinery, communicating with engineered *E. coli* bacteria through the *quorum sensing* molecule (3-oxohexanoyl)-L-homoserine lactone (3OC6-HSL). 3OC6-HSL is one of the signaling acyl-homoserine lactones which are produced by specific bacterial synthases that form a covalent bond between a lactone ring derived from S-adenosylmethionine (SAM) and an acyl chain transferred from acyl carrier protein

(ACP). 3OC6-HSL is synthesized by LuxI that catalyzes the synthesis of N-(3-Oxohexanoyl)-L-homoserine lactone in *Vibrio fischeri*. 3OC6-HSL binds to LuxR activator of transcription which drives the expression of the bioluminescence related gene cassette in cooperation with the bacterial RNA polymerase. 3OC6-HSL synthesized by the artificial cells induces engineered bacteria to synthesize and release a pore forming protein which in turn permeabilizes cargo liposomes encapsulating glucose. Glucose acts as substrate of proteinosomes made of glucose oxidase. Glucose oxidase was modified in in order to carry the hydrophobic polymer poly(N-isopropylacrylamide) (PNIPAAm). The resulting amphipathic macromolecules form Pickering emulsions around water-in-oil droplets. These structures are stabilized by covalent crosslinking for a stable transfer into water phase where they can be in contact with liposomes. Proteinosomes oxidize glucose to gluconic acid forming hydrogen peroxide. Hydrogen peroxide kills the last player in the network, *E. coli* bacteria.
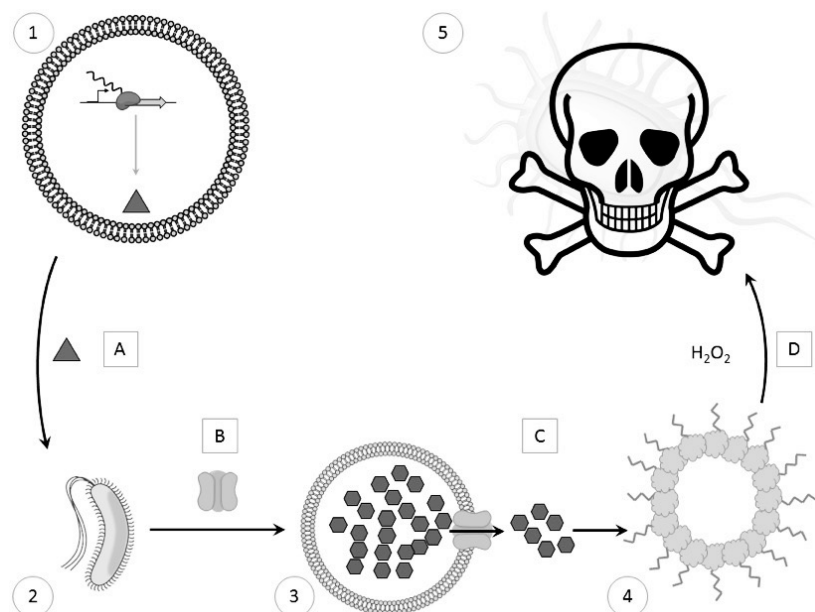
Figure 1. Schematic representation of artificial cells-engineered E. coli cells communication network. The communication network starts with lipid-based artificial cells (**1**) synthesizing and releasing 3OC6-HSL (**A**) to induce engineered E. coli (**2**). E. coli is transformed with two plasmids that allow the 3OC6-HSL-dependent synthesis and release of a pore forming protein (**B**). The released pore forming protein permeabilizes cargo liposomes (**3**) encapsulating glucose (**C**). The released glucose is substrate for glucose oxidase-based proteinosomes (**4**). The oxidation reaction leads to the increase of hydrogen peroxide (**D**), ultimately killing a second population of fluorescent protein expressing engineered E. coli (**5**). E. coli death is monitored by colony forming unit count. Credit: Dario Cecchi.

Here is presented the partial characterization of the second step of the artificial cells-natural cells communication network (Figure 2). First, an *in vitro* test of liposomes permeabilization activity of three pore forming proteins, aHemolysin, Lysteriolisin-O and Perfringolysin-O is presented. Pore forming activity was tested on different liposomes to assess the most suited lipid ratio for the efficient encapsulation and release of a molecular cargo. Second, the 3OC6-HSL-induced cell death was tested. Finally, a demonstration that *in vivo* bacteria-induced liposomes permeabilization is given.
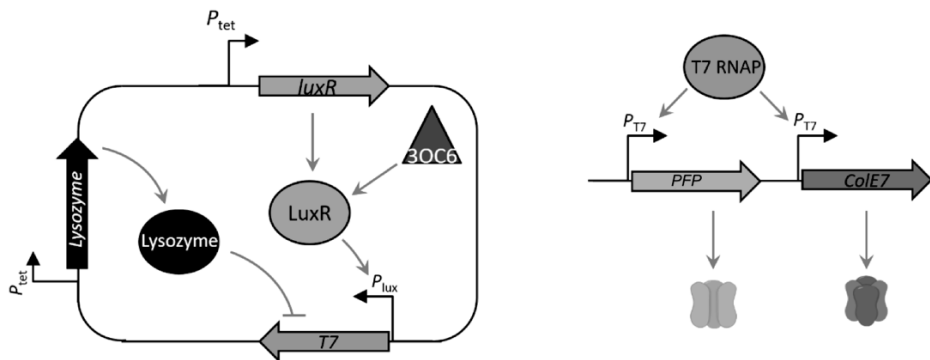
Figure 2. Schematic representation of the plasmid constructs for the engineering of the E. coli cells. *E. coli bacteria depicted as image 2 in Figure 1, induce the permeabilization of cargo liposomes upon 3OC6-HSL induction. The inducer molecule is sent by upstream artificial cells. E. coli bacteria are transformed with two plasmids with different origin of replication and antibiotic resistance gene. On the **left**, the first construct provides information for LuxR activator constitutive production. When 3OC6-HSL is present, LuxR activates the transcription of T7 RNA polymerase gene, coded behind the luxR promoter. The T7 lysozyme system is implemented to neutralize basal expression of T7 RNA polymerase for a tighter expression control. On the right, the second plasmid carries two T7 promoters driving the expression of a colicin (ColE7) and a pore forming protein (PFP). T7 RNA polymerase production results in the transcription of these two genes. The colicin is responsible for the death of bacteria and the resulting release of the PFP in the medium. Free PFP can reach and permeabilize cargo liposomes. Credit: Dario Cecchi.*

3.2. Results

***In vitro* screening of liposomes permeabilization**

In order to achieve an efficient permeabilization of cargo liposomes, different cholesterol contents for the membrane were screened. Liposomes were prepared with the FDEL technique using different POPC:cholesterol ratios but keeping the final lipid molarity. Dried liposomes were prepared with 80% POPC-20% cholesterol, 60% POPC-40% cholesterol and 40% POPC-60% cholesterol with a constant final lipid concentration of 12 mM. Liposomes were encapsulating calcein at self-quenching concentration (80 mM) in order to assess membrane permeabilization by monitoring calcein fluorescence. The *in vitro* permeabilization activity of aHL, LLO and PFO was tested by synthesizing each pore forming protein using the homemade S30 Extract cell-free transcription-translation system, in presence of the calcein encapsulating liposomes.

The plasmids used to template the reaction allowed for constitutive expression of LuxR activator of transcription which, in presence of 3OC6-HSL, was driving the expression of the pore forming protein (aHL, LLO or PFO). In this way, it was also possible to evaluate the performance of the LuxI/LuxR system in terms of expression regulation tightness in this context.
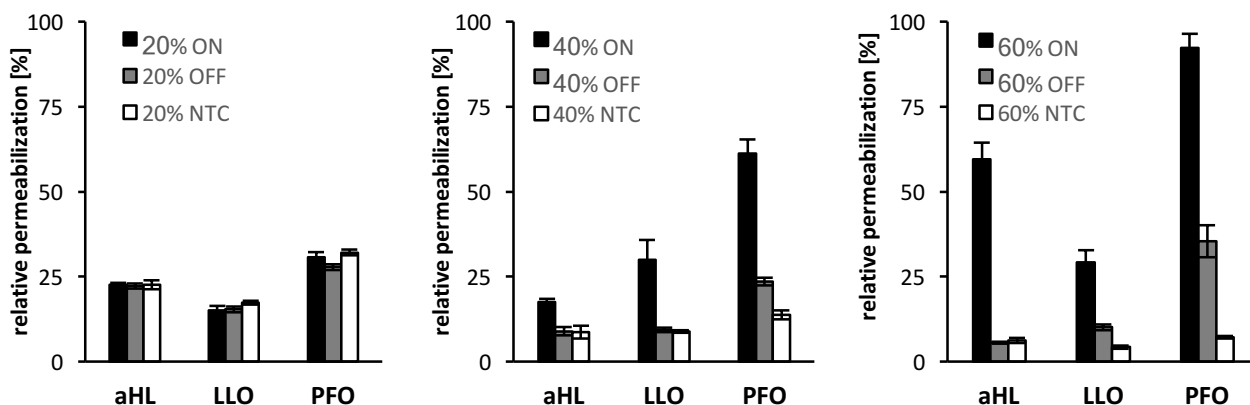
Figure 3. Pore forming protein-dependent in vitro liposomes permeabilization.
*S30 Extract reactions with templates for 3OC6-HSL-inducible synthesis of aHL (NT001A), PFO (NT002A) and PFO (DC171A) were run in presence of liposomes encapsulating 80 mM calcein. Each bar represents the maximum liposomes permeabilization observed in the corresponding reaction. Permeabilization levels were normalized against the ones obtained in a positive control reaction added with 0.5% TritonX-100 where all the liposomes were assumed to be disrupted. Shown are data of the experiments performed with 20% cholesterol liposomes (**left**), 40% cholesterol liposomes (**center**) and 60% cholesterol liposomes (**right**). Each S30 Extract reaction provided with a plasmid template for the synthesis of the pore forming proteins was induced with 1 μM 3OC6-HSL (**black bars**) or non-induced (**grey bars**). Non-template controls were run to assess background permeabilization levels (**white bars**). Reactions were run in triplicate at 30 °C and calcein fluorescence data was acquired with Rotor-Gene Q 6plex (Qiagen) (excitation: 470 ± 10 nm; emission: 510 ± 5 nm).*

A general correlation was observed of increased stability of liposomes (lower NTC permeabilization levels) with higher cholesterol content. Among the three pore forming proteins, PFO seems the best performing one, especially on higher cholesterol liposomes. Leakage in LuxI/LuxR expression regulation system was observed.

While screening pore forming permeabilization efficiency, additional reactions with a template for RFP synthesis were run in duplicate with the same settings *i.e.* in presence of liposomes with different membrane compositions (POPC and 20, 40 or 60% Cholesterol). RFP fluorescence was measured and accounted for two controls at once. First, S30 Extract functioning was checked for possible biases due to the presence of liposomes with different membrane compositions (Figure 4). Second, the leakage of

calcein from liposomes was monitored. In such reactions indeed, calcein release should not occur as observed in the NTC reaction.
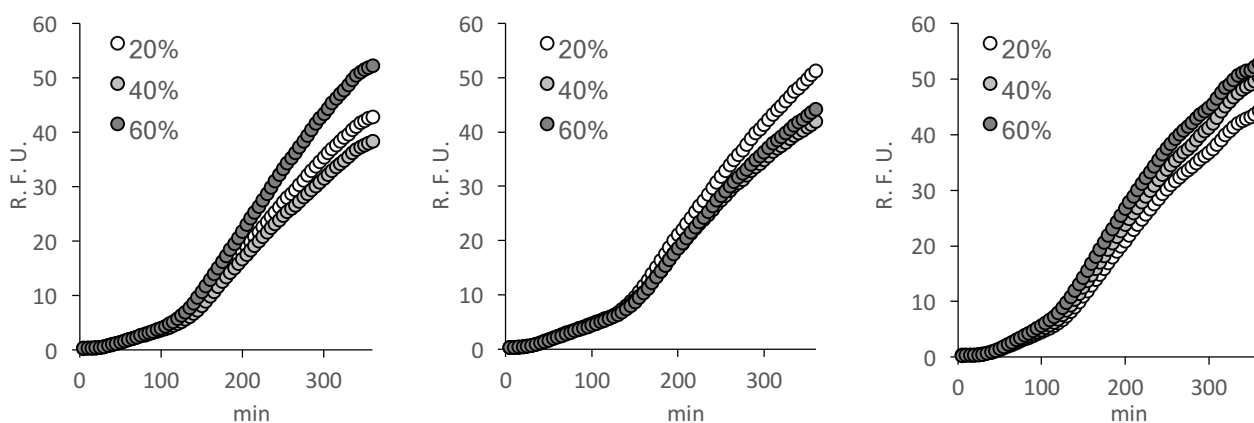

Figure 4. Control reactions for in vitro calcein release assay. *S30 Extract in vitro synthesis of RFP was performed in presence of calcein liposomes to verify the integrity of the reaction. Template used was DC044A, bearing RFP coding sequence behind E. coli constitutive pTac promoter. Synthesis of RFP in presence of different liposomes was performed alongside aHL experiment (**left**), LLO experiment (**center**) and PFO experiment (**right**). Reactions were run in duplicate at 30 °C and RFP fluorescence data was acquired with Rotor-Gene Q 6plex (Qiagen) (excitation: 585±5 nm; emission: 610±5 nm).*

The S30 Extract RFP control reactions performed approximately the same throughout all the experiments. Therefore, the presence of different liposomes did not affect *in vitro* transcription-translation.

E. coli 3OC6-HSL-induced death

To test the system for the bacteria-mediated permeabilization of cargo vesicles, the first step of the mechanism, *i.e.* 3OC6-HSL-induced cell death, was assayed (Figure 5). *E. coli* cells were transformed with two plasmid constructs. The first plasmid allows for T7 RNA polymerase expression in a 3OC6-HSL-inducible manner and implements the pLysS system for neutralizing the leaky expression of the polymerase. The second plasmid has

two T7 promoters driving the expression of the pore forming protein and the colicin. The colicin accounts for the killing of bacteria and resulting release of the pore forming protein, which in turn is responsible for the final permeabilization of the cargo liposomes. The plasmids have different origin of replication to ensure correct propagation of both and carry different antibiotic resistance genes for the stringent selection of co-transformed bacteria. Bacteria were grown and induced with 3OC6-HSL. The aim of this experiment was to verify that bacteria were actually dying upon the addition of the inducer molecule.
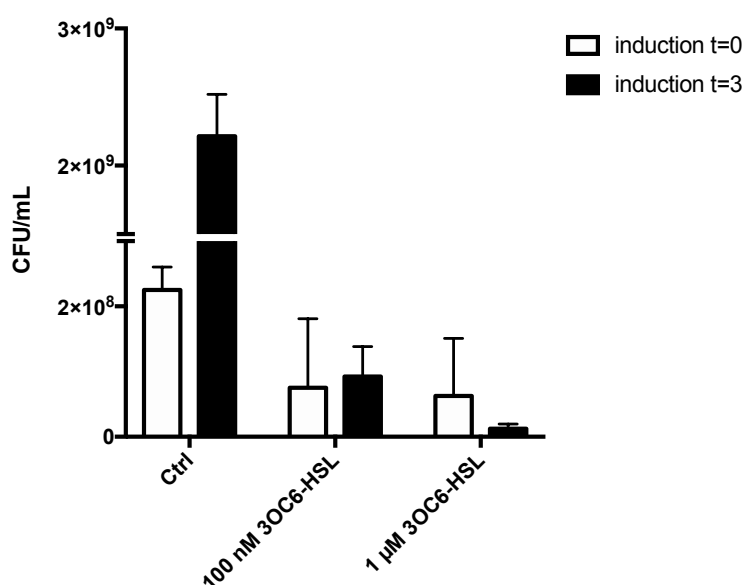

Figure 5. Monitoring of engineered E. coli death induced by 3OC6-HSL. TOP10 E. coli cells were transformed with both DC174C and DC171A plasmid vectors, providing information for 3OC6-HSL-dependent T7 RNA polymerase synthesis and T7 RNA polymerase-dependent expression of PFO and the colicin, respectively. Bacteria were induced with either 100 nM of 1 μM 3OC6-HSL. Right after induction and 3 hours after induction, serial dilutions were prepared of the cultures and plated on LB plus antibiotic agar plates. Colonies were counted and colony forming units/mL was calculated for each culture.

After 3 hours of induction the colony forming units of the non-induced control increases. Colony forming units count of induced cultures after 3 hours is either the same

as before (100 nM 3OC6-HSL) or even lower (1 μM 3OC6-HSL) meaning that most of the cells died upon induction.

In vivo permeabilization of calcein vesicles

To finally show that induced co-transformed bacteria could cause the permeabilization of cargo vesicles, an *in vivo* calcein release assay was performed. Bacteria were transformed with the two plasmids as described before and self-quenching concentration vesicles were added to the culture. After 3OC6-HSL induction, cells were incubated overnight and calcein fluorescence was measured on collected supernatant samples (Figure 6)
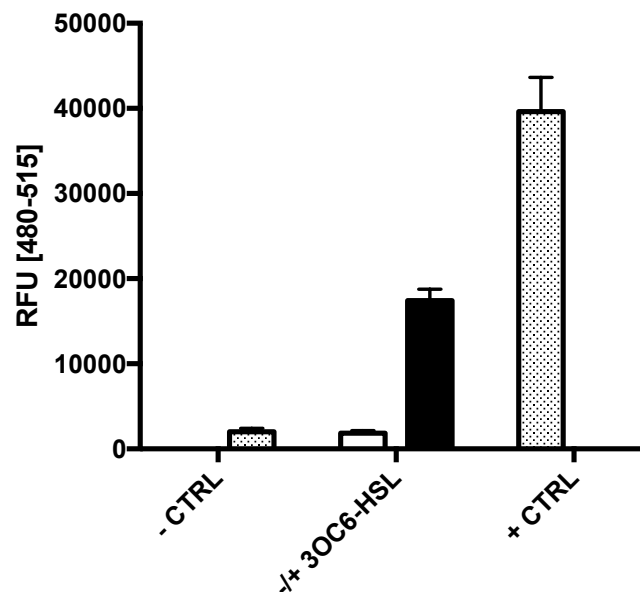

*Figure 6. In vivo permeabilization of calcein liposomes. TOP10 cells were transformed with transformed with both DC174C and DC171A plasmid vectors, providing information for 3OC6-HSL-dependent T7 RNA polymerase synthesis and T7 RNA polymerase-dependent expression of PFO and the colicin, respectively. 80 mM calcein encapsulating liposomes were prepared and mixed with the bacterial culture. Culture was split and either induced (**black bar**) or not (**white bar**) with 100 nM 3OC6-HSL. Bacteria were incubated o/n and calcein fluorescence was measured of a sample from the collected supernatant. Controls are represented as **dotted bars**. Positive control was the addition of 0.3% Triton X-100. Negative control was the addition of LB medium supplemented with dimethyl sulfoxide (DMSO) to a final concentration of 1%. DMSO control was*

Induced engineered bacteria can permeabilize cargo liposomes upon inducer molecule induction. Addition of 3OC6-HSL induced the expression of T7 RNA polymerase which, in turn, drives the expression of the colicin and of the pore forming protein. Dead bacteria released the synthesized pore forming protein, which ultimately permeabilized calcein-encapsulating liposomes.

3.3. Discussion

The proposed approach for the creation of a communication network between artificial cells and engineered bacteria involves the design and characterization of each one of the steps depicted in Figure 1. In this work, the characterization of one step is presented. The step which was taken into account is the one in which engineered bacteria (Figure 1, element 2) are induced by 3OC6-HSL to release a pore forming protein to provoke the release of glucose from cargo liposomes (Figure 1, element 3).

The permeabilization activity of three different pore forming proteins synthesized *in vitro* using the S30 Extract protein synthesis system was tested on liposomes with different membrane compositions to assess the best performing setting. Although the actual concentrations and ratios of lipids are not clearly defined in rehydrated liposomes, it was clear that the more cholesterol present in the membranes, the higher the activity of the pore forming proteins. LLO and PFO belong to the cholesterol-dependent cytolysin family[4,5] and were expected to perform better on membranes with higher cholesterol content. On the other hand, αHL is reported to recognize different docking site molecules on eukaryotic cell surfaces like metalloproteinases, in particular ADAM10[6]. Nevertheless, cholesterol depletion has already been observed to abrogate the binding of αHL to host cell membranes. The proposed mechanism is that low affinity binding moieties can assume the role of high affinity binding sites due to their spatial arrangement in the membrane[7]. The activity of all the three pore forming proteins is visibly increased with higher cholesterol content with the exception of LLO which performs better on 40% cholesterol liposomes rather than on 60% cholesterol liposomes. It has been reported that pre-incubation with cholesterol can inhibit the activity of cholesterol-dependent cytolysins[8–10]. Therefore, a possible explanation of this counter intuitive effect is that the high concentration of cholesterol employed for the preparation of liposomes may have led to a certain amount of free cholesterol molecules, sufficient for the inhibition of the pore forming protein activity. In the particular case of LLO, too much cholesterol should be avoided in the preparation of liposomes. The highest permeabilization activity was observed when using PFO on 60% cholesterol liposomes, where the calcein release levels were close to the ones obtained with the addition of Triton X-100 detergent.

Each plasmid vector used to template the S30 *in vitro* cell-free protein synthesis enables the expression of the forming protein in a 3OC6-HSL-dependen fashion. Using this plasmid, it was possible to evaluate the expression regulation tightness of the LuxI/LuxR system. The regulation system shows a considerable leakage of expression in absence of the inducer molecule. The effect is more noticeable when permeabilizing liposomes with higher cholesterol content. The leakage in expression control was confirmed *in vivo* in the lab (data not shown) suggesting that the LuxI/LuxR system may not suited for achieving a tight 3OC6-HSL-inducible release of pore forming protein using *E. coli*.

In order to achieve a better expression control, a new regulation system was designed by Dario Cecchi that implements T7 RNA polyemerase. The new system consists of two plasmid constructs. The first construct is based on the pLysS vector and allows for the expression of T7 RNA polymerase in a 3OC6-HSL-inducible manner. T7 lysozyme coding sequence is present in the construct and its expression leads to the inhibition of basal levels of T7 RNA polymerase. The second plasmid carries the coding sequences of the pore forming protein and of ColE7 bacteriocin, both regulated by a dedicated T7 promoter (Figure 2). Here the system was tested for functioning. The chosen pore forming protein was PFO (highest permeabilization activity observed) and the cargo vesicles were prepared with 60% cholesterol (best setting for higher permeabilization). First, the inducible activity of ColE7 bacteriocin was tested by colony forming units count. Bacteria previously transformed with both the plasmids were responsive to 3OC6-HSL induction and showed to stop their growth and die. Then, the release of pore forming protein and the following permeabilization of cargo vesicles was tested. Calcein was encapsulated in liposomes and incubated with 3OC6-HSL-responsive bacteria previously transformed with the two plasmid constructs and bacteria were induced to synthesize PFO and ColE7. Calcein was released when the bacterial culture was induced with 3OC6-HSL while no calcein release was observed when the inducer molecule was not added.

These observations suggest that the system is working. It must be said that the bacteria-induced permeabilization of calcein vesicles did not give positive results in the case of time points earlier than 16 hours. This is an indication of good stability of the cargo vesicles which are still intact if no pore forming protein is synthesized and released

by bacteria. Nevertheless, concerns arise regarding the final assembly of the whole network. The downstream step in the communication flow involves glucose oxidase proteinsomes which are required to maintain their functionality until the glucose will be released from the cargo liposomes. Further tests must be performed to evaluate the stability of proteinosomes. Moreover, the presence of glucose in the network medium must be taken into account since it could serve as proteinosomes substrate for the formation of hydrogen peroxide ahead of the induced release of the liposomes-stored glucose.

3.4. Materials and methods

Preparation of calcein liposomes

The Freeze-Dried Empty Liposomes (FDEL)[11] method involves the formation of a thin lipid film after the evaporation of the organic solvent where lipids are dispersed, typically chloroform. The film is resuspended in water to allow for the formation of vesicles containing multiple lipid bilayers and homogenized by mechanical stirring or extrusion. Vesicles are then lyophilized and later resuspended with the aqueous solution to be encapsulated. 1-palmitoyl-2-oleoyl-*sn*-glycero-3-phosphocholine (POPC) and cholesterol stocks were dissolved in chloroform to 10 mg/mL. The desired amount was transferred into a glass round bottom flask and chloroform was evaporated using a rotary evaporator (Buchi). The lipid mixtures were resuspended in distilled water to a final concentration of 12 mM with different molar ratios of POPC and cholesterol. Liposome mixtures were homogenized for 1 min with T10 basic ULTRA-TURRAX disperser set at power 4. The solution was split into 100 µl aliquots in 2 mL tubes, flash-frozen in liquid nitrogen and dehydrated overnight with a benchtop vacuum concentrator (Labconco). Aliquots were stored at -20°C.

A total of 200 µL of calcein solution in water (80 mM, self-quenching concentration) was used to resuspend the lipid film of 4 dried liposomes stocks by vortexing. Resuspended liposomes were extruded 11 times through a 200 nm cut-off polycarbonate membrane using Mini Extruder (Avanti). Liposomes were purified from the non-encapsulated dye by gel filtration on a Sephadex G-50 matrix (GE Healthcare) using water as mobile phase.

3.5. References

1. Caschera, F. & Noireaux, V. Synthesis of 2.3 mg/ml of protein with an all Escherichia coli cell-free transcription–translation system. *Biochimie* **99,** 162–168 (2014).

2. Noireaux, V. & Libchaber, A. A vesicle bioreactor as a step toward an artificial cell assembly. *Proc. Natl. Acad. Sci.* **101,** 17669–17674 (2004).

3. Huang, X., Li, M. & Mann, S. Membrane-mediated cascade reactions by enzyme–polymer proteinosomes. *Chem. Commun.* **50,** 6278–6280 (2014).

4. Bavdek, A. *et al.* PH dependence of listeriolysin O aggregation and pore-forming ability. *FEBS J.* **279,** 126–141 (2012).

5. Reboul, C. F., Whisstock, J. C. & Dunstone, M. A. A New Model for Pore Formation by Cholesterol-Dependent Cytolysins. *PLoS Comput. Biol.* **10,** (2014).

6. Wilke, G. A. & Wardenburg, J. B. Role of a disintegrin and metalloprotease 10 in Staphylococcus aureus - hemolysin-mediated cellular injury. *Proc. Natl. Acad. Sci.* **107,** 13473–13478 (2010).

7. Valeva, A. *et al.* Evidence That Clustered Phosphocholine Head Groups Serve as Sites for Binding and Assembly of an Oligomeric Protein Pore. *J. Biol. Chem.* **281,** 26014–26021 (2006).

8. Nöllmann, M., Gilbert, R., Mitchell, T., Sferrazza, M. & Byron, O. The role of cholesterol in the activity of pneumolysin, a bacterial protein toxin. *Biophys. J.* **86,** 3141–51 (2004).

9. Watson, K. C., Rose, T. P. & Kerr, E. J. Some factors influencing the effect of cholesterol on streptolysin O activity. *J. Clin. Pathol.* **25,** 885–91 (1972).

10. Jacobs, T. *et al.* Listeriolysin O: Cholesterol inhibits cytolysis but not binding to cellular membranes. *Mol. Microbiol.* **28,** 1081–1089 (1998).

11. Kikuchi, H. *et al.* Gene delivery using liposome technology. *J. Control. Release* **62,** 269–277 (1999).

Chapter 4.

A microfluidic dialysis chip for synthetic biology

4.1. Introduction

Microfluidics

Microfluidics is a field dealing with the design, production and application of devices or processes involving volumes of liquids in the nanoliter or picoliter scale. In the last couple of decades microfluidics is taking advantage of new microfabrication technologies coming from the microelectronics and semiconductor industry. Applications are many and diverse such as blood-cell-separation equipment, biochemical assays, protein crystallography, chemical synthesis, genetic analysis, production of quantum dots and drug screening devices through droplet-based microfluidics. The advantages of using a microfluidic device are to stream-line complex assay protocols and to substantially lower the sample volume, thus reducing reagents consumption and maximizing the amount of information per valuable sample.

Although the concepts of miniaturization and parallelization usually brought to an advance in technology, microfluidics largely did not impact the way scientific research is generally done. The most likely reason why microfluidics is not widely implemented in every biology lab and more in general in other science fields, is that technology users want technology to be simple, cheap and easy. Biology researchers have more than enough problems to deal with by simply working in the lab and no time to spend learning how to make and use microfluidic devices. On the other hand, technology developers, especially in universities, are often not interested in solving real problems and they want technology to be technically cool.

Working at the microscale means that fluid dynamics are different from the macroscale ones. For instance, surface tension and capillary forces become much more important than gravity. Liquid flow in a microfluidic channel is laminar and convective mixing does not occur thus enabling predictable diffusion kinetics (laminar vs turbulent flow). These properties have been exploited for a variety of tasks like passively pumping of fluids in micro-channels, precisely patterning surfaces with different samples[1], filtering analytes[2] and forming monodisperse droplets in multiphase stream for different applications[3]. These are just a few problem examples that microfluidics attempted to solve. Over the years, the development of microfluidic solutions for biomedical research has been embraced by engineers that analyzed different materials and fabrication processes.

The material the device is built with has to interact with a large amount of different and complex liquid samples. For this reason, in microfluidics there is an optimally suited material for any given tasks and there is not a single universal solution. Most of the devices were at the beginning fabricated with silicon[4] and glass,[5] using clean-room techniques adapted to microfluidic devices fabrication. This choice was due to convenience since techniques and facilities were already in place; moreover, the first microfluidic applications were focused largely on electrophoretic phenomena and glass was the best option. Although these materials were well suited for some applications, with microfluidics moving towards biology research, the use of glass and silicone limited the development and adaptation of the technology to biology research. The need for cheaper and more accessible materials was met by elastomeric micro-molding techniques developed by Bell Labs in the 1970s[6] which were then applied to microfluidics and cell biology in the 80s[7]. In the early 2000s, Whitesides described a procedure that made it possible to design and fabricate microfluidic systems in polydimethylsiloxane (PDMS) in less than 24 hours[8]. This crucial step in microfluidics was well represented by the growth of the number of publications[9]. Also, thermoplastics such as polystyrene have been tested for the fabrication of microfluidic devices [8,10,11] although the use of these materials does not come without limitations[12]. Biology has a long history of polystyrene usage for cell culture since this thermoplastic eliminates some issues associated with PDMS and makes handling and packaging easier. In addition to thermoplastic materials, also cheap and destructible materials such as paper, wax and cloth have been tested for

point-of-care application in low-resource settings. The paper-based analytical devices (μPADs) have the advantage of being easily incinerated, making them ideal for settings where there is no disposal for biological samples. These devices are the expansion of lateral flow assays such as pregnancy strip test. Indeed, this kind of tests uses patterned hydrophilic cannels where the sample can passively wick through by capillary force, often inducing a colorimetric readout. μPADs are becoming increasingly sophisticated[13] and in recent studies it has been shown how paper can be used as vehicle to embed, store and operate synthetic gene circuits in a reproducible manner by freeze drying a cell-free gene expression system along with DNA on a piece of paper[14].

Rather than solely relying on PDMS for device fabrication, the microfluidic community is moving towards alternatives that solve problems in preforming cell biology and diagnostic assays. However, using a different material often requires a re-thinking of components design. For instance, valves and pumps, often present in a PDMS device, are not easy to implement in thermoplastic devices and this will require creative new approaches from engineers to create powerful Lab-on-a-chip devices.

PDMS

Polydimethylsiloxane is a mineral-organic polymer that belongs to a group of compounds commonly referred as silicones. The formula for PDMS is $CH_3[Si(CH_3)_2O]_n Si(CH_3)_3$, where n is the number of repeating monomer $[Si(CH_3)_2]$ units. Apart from microfluidics, PDMS is used as a food additive (E900), in shampoos and as antifoaming agent in beverages. For the fabrication of microfluidic devices, liquid PDMS is mixed with a cross-linking agent that renders it a hydrophobic elastomer.

PDMS has several advantages compared to silicon and glass. First of all, the set-up for fabricating a small number of PDMS devices is relatively cheap. Also, PDMS can be easily treated to turn the hydrophobic surface into a hydrophilic type of surface,[15] and PDMS can reversibly or (in some cases) irreversibly be bonded to plastic, glass, PDMS itself and other materials. This is possible through plasma treatment, a process that changes the polymer surface chemistry and produces silanol terminations (SiOH) on PDMS surfaces that can then react with glass or chemical solutions. PDMS is a

transparent silicon, allowing for the use of microscopy to monitor the sample. Finally, this polymer is generally considered as biocompatible and flexible. The elasticity of PDMS is probably the most important quality of the material since it allows for an easy removal from the delicate master mold to obtain many replicates of the chip. For this reason, PDMS devices are considered as single-use chips, eliminating contamination between analyses. Furthermore, the elasticity property of PDMS allows for valving and actuation[16]. The pressure-driven deformation of the material can be exploited to clog or release liquid flows into two-layer microsystems. These pneumatic micro-valves were introduced for the first time in the 2000 almost simultaneously by Stephen's Quake group in Stanford and Hosokawa and Maeda in Japan. In this way, thousands of micromechanical valves can be placed in a single device, enabling control over the biological content[17].

Despite all these beneficial properties, there are also several limitations for implementing the material in biomedical research. For instance, it has been shown how PDMS can leak un-crosslinked oligomers from the curing process into solution,[18] which often requires additional treatments to reduce this potentially harmful effect. Additionally, PDMS as a hydrophobic material, can absorb small hydrophobic molecules, which can affect critical cell signal dynamics or impair *in vitro* reactions[19]. Furthermore, since PDMS is gas permeable, evaporation can occur during experiments. This can be detrimental for essays especially when low volumes are involved and when osmolarity matters[20]. In conclusion, PDMS is perfect for prototyping new chip design concepts; however, researchers have also to take into account a number of limitations and precautions while designing and performing experiments.

Rapid prototyping begins with the printing of the chip design onto a transparent film with a high-resolution printer. This transparency is used as a mask in contact photolithography and a layer of resist. In this work, the masks used are made of photo-curable epoxy, SU-8, radiated with UV light to induce polymerization of the exposed regions. After removing the un-polymerized photoresist, a positive relief of the design remains on the silicon wafer; this structure acts as a master mold for casting the PDMS chip. In general, the process can be repeated to obtain multilayer structures. In this case, the un-polymerized photoresist is not removed and a second layer of photoresist is spun

on top of the first. Moreover, a second mask needs to be finely aligned and then, as described above, the photoresist is polymerized. Finally, by dissolving the un-polymerized photoresist it leaves multilayer channels structures. The surface of the resulting wafer can be treated with a silane containing fluorinated functional group to facilitate the PDMS slab removal.

PDMS chips are fabricated by soft lithography using elastomeric polymer molding, a technique which enables rapid prototyping. This process can be carried out in standard laboratory conditions without the need for cleanroom facilities. Using the master mold, a negative relief of the structure in PDMS is made by replica molding. PDMS pre-polymer is poured over the wafer mold, heated to 40 - 80 °C and finally, peeled off from the master. Channel inlets and outlets are created with a hole-puncher. The channels are usually sealed (reversibly or irreversibly) against a flat substrate[21]. This cheap and time-saving procedure allows for the design, fabrication and testing of new channel configurations. This is important in the prototyping stage of designing microfluidic devices, since several iterations may be needed before obtaining a working design.

Cell-free protein synthesis in microfluidics compartments

The compartmentalization of a transcription-translation system in microfluidic chambers can have different final goals. For example, this approach has been proposed as a good tool for rapid prototyping of genetic circuits. Compartmentalized cell-free *in vitro* systems have the advantage of being completely defined, and the absence of a cell wall leads to an open system allowing continuous monitoring and specific adaptation of the reaction parameters.

Compartmentalized transcription-translation in microfluidic systems can be exploited for the high-throughput production of different proteins[22]. This kind of device can significantly reduce reagent consumption compared to commercially available cell-free protein synthesis kits and can be used as a straightforward strategy for parallelized high-throughput applications using standardized equipment in drug discovery. Microfluidic bioreactors have also been proposed to facilitate the on-demand production

of therapeutic proteins for medicines and biopharmaceuticals at the point-of-care. Making these miniature factories cell-free should simplify the process and lower costs[23].

Here is presented a variation of an existing microfluidic dialysis device that was prepared to run an array of cell-free protein synthesis reactions in continuous exchange mode in which the mechanism and mounting is based on another device developed for birefringence visualization in microliter samples[24]. The original chip allowed for the efficient study of phase transitions, such as crystallization and gelation[24]. Here, a similar system is exploited to build a microfluidic platform to test chemical communication between bacteria and between different transcription-translation systems. The microfluidic device is characterized by two different chip designs. The storage layer allows for the compartmentalization of an aqueous sample into wells separated by oil. The reservoir layer allows for a continuous flow of aqueous sample. The two layers are separated by a dialysis membrane permeable to water and small water-soluble molecules. To restrict the communication to a part of the storage layer wells, a Teflon foil with partially aligned holes was also exploited leading to the establishment of ON and OFF states for the storage layer wells.

4.2. Results

Polypropylene chip preparation and dialysis chip mounting

The original dialysis chip was characterized by both storage and reservoir layers made of PDMS. The mounting of the original sandwich dialysis chip was not trivial and required high concentrations and delicate touch for the correct alignment of the multiple components. Moreover, once reached the perfect alignment, tightening the screws in a slightly sub-optimal way could easily lead to uneven pressure distribution, distortion of the storage layer and leakage of the sample. In sight of a more accessible procedure, it was explored the possibility of using polypropylene in place of PDMS for the storage layer of the sandwich. Polypropylene is more rigid than PDMS. Therefore, polypropylene could lead to a device that is less distortable, thus avoiding leakage.

Since polypropylene is a solid polymer at room temperature, a standard casting could not be performed like in the case of PDMS. In order to prepare a polypropylene chip, the plastic had to be softened by heat and put in close contact with the mold in order for the features to be faithfully printed on the hot plastic. In this particular case, silicon molds could be likely damaged by the peeling of the cooled, solid polypropylene. A PDMS mold was used instead. A silicon wafer mold with positive features was designed and used for the casting of a negative-featured PDMS chip. This acted as mold for the production of positive-featured final polypropylene chips (Figure 5).

Polypropylene was obtained directly from petri dishes given the ~1 mm thickness, ideal for handling. The dish walls were removed with pliers, then a scalpel was used to carve grooves on the plastic to allow the precise cracking of the disc to finally obtain small squares (~2 cm x 2 cm) as shown in Figure 1.
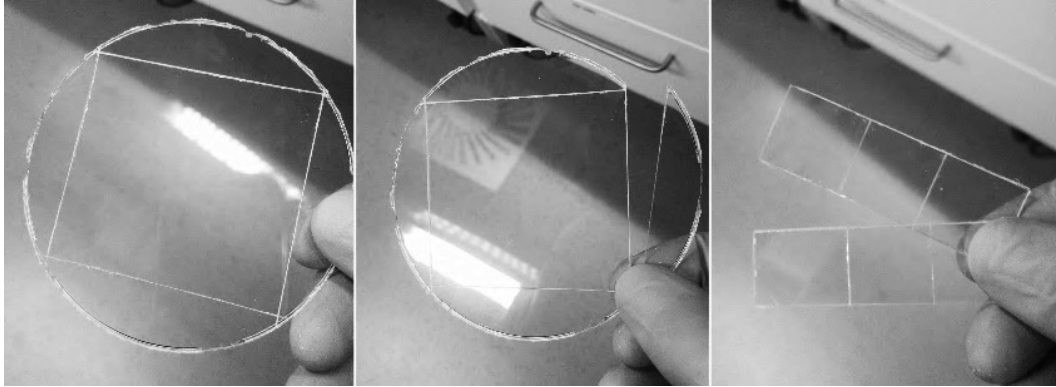
Figure 1. Preparation of the plastic unit for the polypropylene chip printing.
The polypropylene squared pieces for the chip following printing were obtained by cracking the bottom of a petri dish alongside scalpel-carved grooves.

To print the reliefs on the polypropylene, the squared unit was placed in contact with the feature face of the PDMS mold after both the surfaces were previously carefully cleaned. Two glass slides were placed over the plastic side and beneath the PDMS side. The resulting "cheeseburger" (where the glass slides are the bread, the plastic is the cheese and the PDMS is the burger) was pressed with two double clips. The glass slides ensured an even distribution of pressure exerted by the clips (Figure 2a and 2b). Before proceeding, the PDMS features were inspected with a stereo microscope to verify that excess pressure was not exerted by the clips. In fact, too much pressure could squeeze and stretch the features of the PDMS, resulting in distorted printing on the polypropylene (Figure 3). The apparatus was incubated on a heating plate set to 200 °C for 1 h. The apparatus was cooled down at room temperature and the PDMS mold peeled off the printed polypropylene chip (Figure 2d).
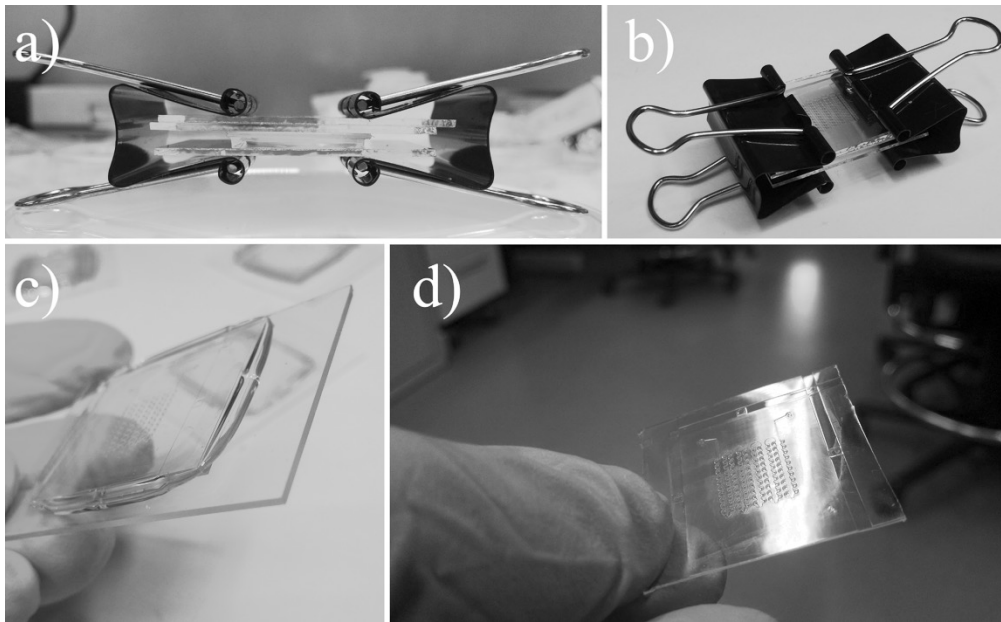
Figure 2. Printing of the features on the polypropylene unit. a), b) *The polypropylene unit was pressed against the PDMS mold with double clips. Glass slides were used to spread the pressure on all the chip area evenly. The apparatus was incubated at high temperature to allow the softening of the polypropylene which adapted to the PDMS mold features.* **c), d)** *After cooling down, the PDMS mold was peeled releasing the polypropylene chip with its printed features.*
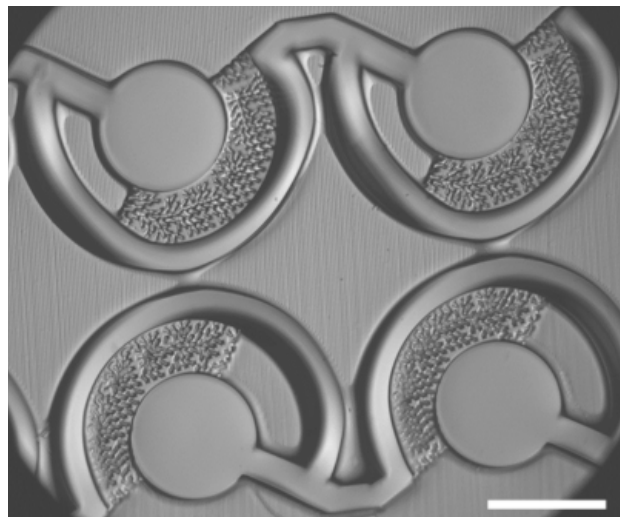

Figure 3. Polypropylene aberrant printing. *The exertion of too much pressure when printing the polypropylene chip resulted in a deformation of the PDMS mold features which were reproduced on the plastic. Scale bar: 400 μm.*

The features on the polypropylene chip were analyzed at the microscope to make sure the channels and wells have been faithfully transferred. Typical plastic chip features look like the ones in Figure 4.
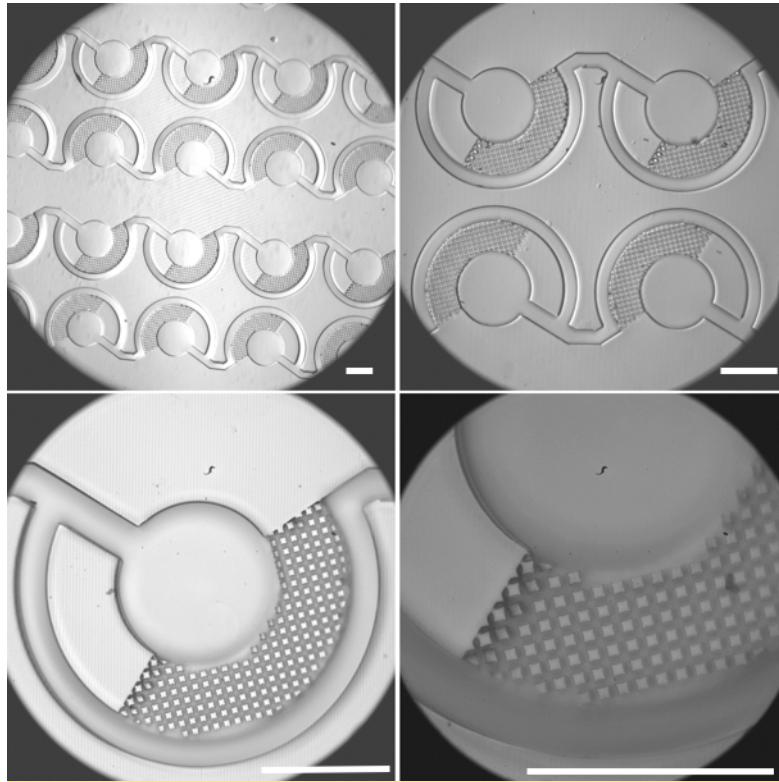

Figure 4. Features printed on polypropylene chip. Represented is a printed polypropylene storage chip. Features can be seen in different magnifications. Wells and pillars are finely reproduced on the plastic. Scale bars: 400 µm.

Since the polypropylene chip has a hard consistency, a different plugging technique was devised. The feature-free surface of the chip needs to be free of holes and tubing. Instead, sample has to be loaded from the side because the two layers will be inserted in the metal frame which will clamp them. PDMS chips are thick and soft enough for holes to be punched to create a sort of pipe allowing for the loading of the sample from a side (Figure 5). Conversely, polypropylene chips are much thinner and hard so that a similar approach would be impossible. Holes were punched through the polypropylene chips along the axis perpendicular to the chip surface. A plain PDMS slab was added in the sandwich with side holes to serve as loading manifold (Figure 5).
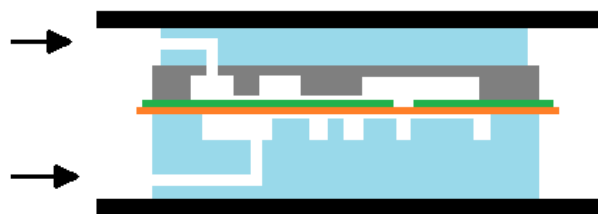
Figure 5. Schematic representation of PDMS and polypropylene chip pluggings. *Both upper and lower surfaces of the chips are not accessible to the loading tubing due to the metal frame scaffold (black). Sample must be loaded from the side. PDMS chips (lower blue part) are thick and soft enough for L-shaped holes to be punched to produce a side-loading manifold. The loading of the polypropylene chip (grey) was achieved with a PDMS slab manifold (upper blue part). Arrows indicate the plugging holes for PFTE tubing. The Teflon foil is depicted in green. The dialysis membrane is depicted in orange.*

Polypropylene chip loading

The loading process described in Materials and Methods section was tested in the new dialysis chip. The water sample-oil interface needs to be well defined for the correct loading and following separation of the sample in the wells. Phospholipids like POPC and egg-PC dissolved in the oil were enough to grant a sharp phase separation but when loading the chip with biological samples some interaction between the oil and the aqueous phase was observed. To address this issue, a fluorinated, synthetic, organic solvent HFE-7500 (Novec) was used in place of mineral oil. To stabilize the interphase, a biocompatible surfactant was used that is the product of the coupling of oligomeric perfluorinated polyethers (PFPE) with polyethyleneglycol (PEG)[25]. Different amounts of surfactant in the fluorinated oil were screened to find the minimum concentration to achieve an effective stabilization of the oil-biological sample interface. 0.2% w/w fluoropolymer surfactant in HFE-7500 fluorinated oil was found to be the minimum and sufficient concentration (Figure 6).
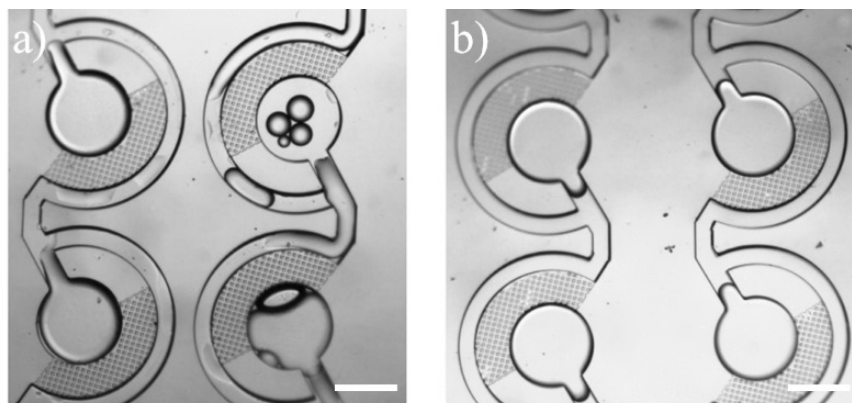
***Figure 6. Fluoropolymer surfactant stabilization of oil-sample interface. a)** 0.1% w/w concentration of PFPE-PEG in HFE-7500 cannot provide interphase stabilization **b)** 0.2% w/w in HFE-7500 fluorinated oil is enough for sample-oil interface stabilization. The biological sample used was a cyan fluorescent protein (CFP). Scale bar: 400 μm.*

E. coli 3OC6 HSL *in vivo* communication

In order to test the applicability of the microfluidics dialysis chip, a bacteria communication experiment was designed. The communication pathway chosen is the one regulating *V. fischeri quorum sensing* bioluminescence, ideal because of its simplicity. The sending part consists in the *quorum sensing* molecule synthase, LuxI. The *quorum sensing* molecule synthesized by LuxI is (3-oxohexanoyl)-L-homoserine lactone (3OC6-HSL). 3OC6-HSL can freely trespass bacteria phospholipid membrane and wall. The receiving part is constituted by the activator of transcription LuxR. Upon binding to 3OC6-HSL, LuxR can activate the transcription of genes behind the luxR promoter element. Moreover the LuxI/LuxR system can be reconstituted in *E. coli*[26] by recombinantly expressing the components. *E. coli* BL21(DE3) pLysS (Promega) was transformed with either a plasmid carrying the LuxI synthase gene downstream of a T7 transcriptional promoter (sending) or with a construct containing a constitutively expressed transcriptional promoter (tet) for *E. coli* RNA polymerase that drives the expression of the LuxR activator and a green fluorescent protein (GFP) reporter controlled by a luxR promoter. The sending *E. coli* can be induced with the galactose analog isopropyl β-D-1-thiogalactopyranoside (IPTG) to express LuxI and thus synthesize 3OC6-HSL. The receiving *E. coli* will constitutively produce LuxR, which activates the expression of GFP in the presence of 3OC6-HSL.

To test the *E. coli*-based LuxI/LuxR system, a flow cytometry experiment was performed. The sending *E. coli* bacteria were grown and LuxI production was induced with IPTG. The 3OC6-HSL-containing supernatant from the culture was then used to induce LuxR-mediated expression of GFP reporter in a receiver *E. coli*. The receiver *E. coli* culture was analyzed by fluorescence-activated cell sorting (FACS) (Figure 7).
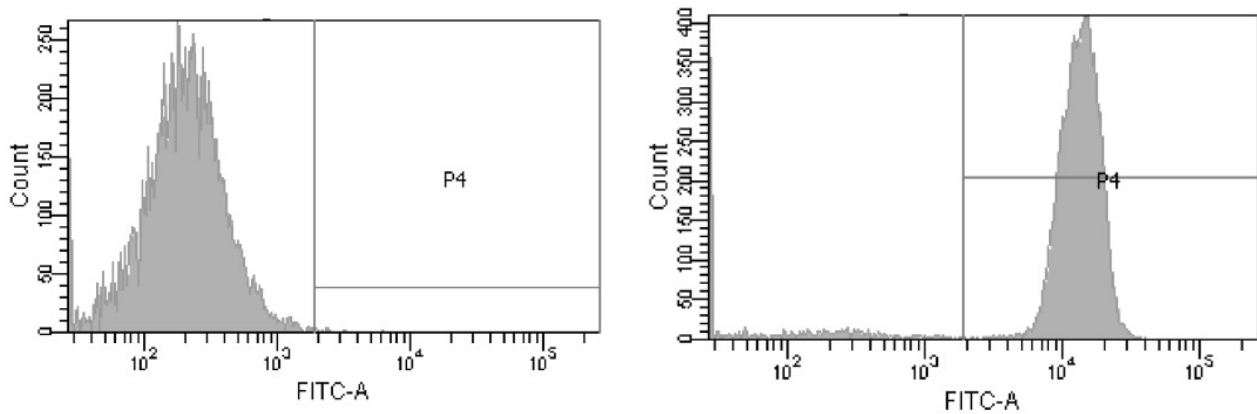

Figure 7. FACS data relative to 3OC6-HSL-dependent GFP reporter expression in engineered E. coli (receiving culture). Supernatant from induced E. coli sending culture was added to the E. coli receiving culture. E. coli receiving culture was then incubated for 1 hour and analyzed. On the left, the result of FACS analysis of receiving bacteria which was added with LB medium instead, as negative control. None of the counts was observed as GFP expressing. On the right, the analysis of the receiving bacteria population added with supernatant of the sending E. coli bacteria. Almost 100% of the population counts were positive for GFP expression when added with supernatant of 3OC6-HSL sending E. coli.

In chip 3OC6-HSL *E. coli* communication

To verify the functionality of the dialysis chip, the 3OC6-HSL communication experiment was run in the two compartments divided by the dialysis membrane and Teflon foil. *E. coli* bacteria transformed with the receiving plasmid allowing for 3OC6-HSL-dependent GFP production were loaded on the storage layer. *E. coli* bacteria transformed with the sending plasmid were induced to produce LuxI synthase and loaded on the reservoir layer. Some of the wells containing the receiving bacteria were not put in contact with the sending part by adjusting the alignment of the Teflon foil (Figure 8, left).
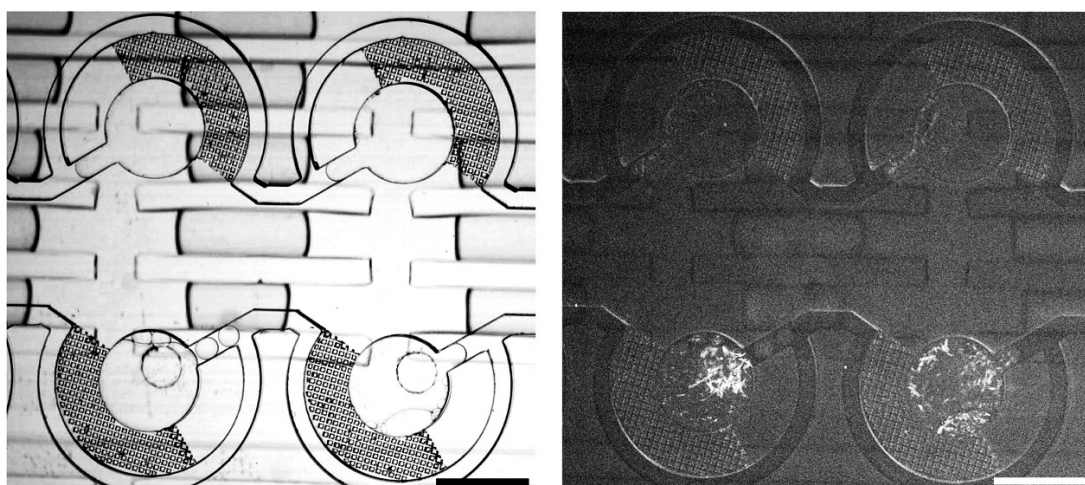

Figure 8. Bacteria bacteria 3OC6-HSL communication inside the dialysis chip. *The dialysis chip was mounted with the Teflon foil partially aligned with the storage upper layer. As a result, some of the circular wells of the storage layer were not in contact with the lower reservoir layer because of the lack of the hole in the Teflon foil. BL21 (DE3) Singles E. coli bacteria transformed with the 3OC6-HSL receiving construct (BBa_T9002) grown till $OD_{600\,nm} = 0.5$ and loaded in the wells and each well was isolated by flushing oil. BL21 (DE3) Singles E. coli bacteria transformed with the 3OC6-HLS sending construct (MC002A) were grown till $OD_{600\,nm} = 0.5$, induced with 0.5 mM IPTG for 1 hour and loaded on the lower reservoir layer of the dialysis chip. Both the syringes flushing oil in the storage and bacteria in the reservoir were connected to syringe pumps (KD scientific) and flow rate of 5 μL/hour was set. Shown are pictures taken after 1 hour of incubation of the chip at room temperature. On the* **left**, *the bright field picture shows two OFF wells on top and two ON wells on the bottom. Holes in the Teflon foil can be seen only in the two bottom wells. On the* **right**, *the fluorescence picture shows GFP expressing bacteria located in the ON wells only. Scale bars: 400 μm.*

S30 *E. coli* Extract 3OC6 HSL *in vitro* communication

To check the feasibility of a completely cell-free version of *quorum sensing* communication in the microfluidics dialysis chip, a homemade *E. coli*-based S30 Extract *in vitro* transcription-translation system was used for the cell-free reconstitution of the 3OC6-HSL sending and receiving parts. Since the S30 Extract had to be used on both the sides of the dialysis chip, a control reaction was run using as template the two plasmid vectors providing the information for both the sending part (pT7-LuxI) and the receiving part (pTet-LuxR; luxR promoter-GFP) (Figure 9).
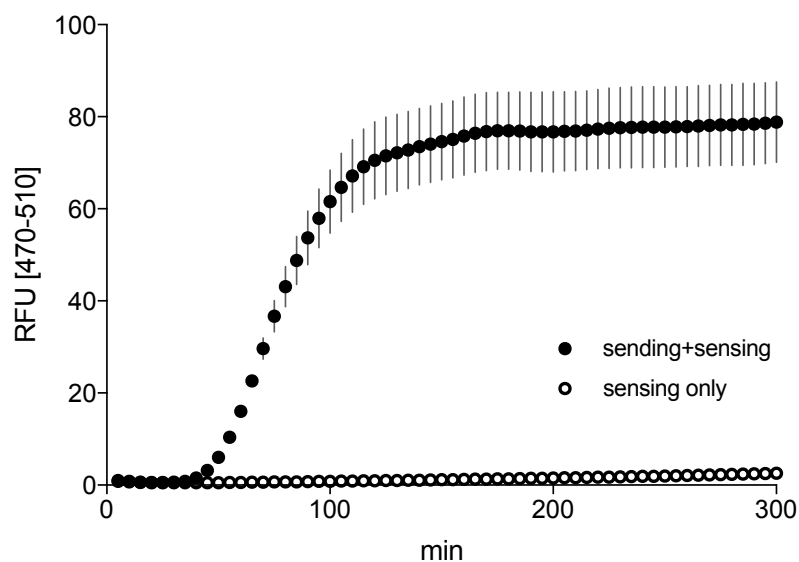

Figure 9. In vitro 3OC6-HSL system verification. *A S30 Extract reaction was run using two plasmid templates MC002A (sending) and BBa_T9002 (receiving) (black circles). The sending template allows for the T7 RNA polymerase-driven expression of LuxI synthase, hence for 3OC6-HSL production. The receiving plasmid allows for E. coli RNA polymerase-driven expression of LuxR and LuxR-mediated expression of GFP. A control reaction was run with the BBa_T9002 receiving template only to assess the background signal (white circles). Reactions were run in duplicate at 37 °C and fluorescence was monitored using Rotor-Gene Q 6plex (Qiagen). GFP fluorescence was acquired with the green channel (excitation: 470 ± 10 nm; emission: 510 ± 5 nm).*

In chip 3OC6-HSL S30 communication

The *E. coli* 3OC6-HSL communication in-chip experiment was fully reconstructed *in vitro.* S30 Extract reactions were loaded in the storage and reservoir layers and provided

with receiving and sending templates, respectively. Some wells containing the receiving reaction were not put in contact with the sending part by adjusting the alignment of the Teflon foil (Figure 10)
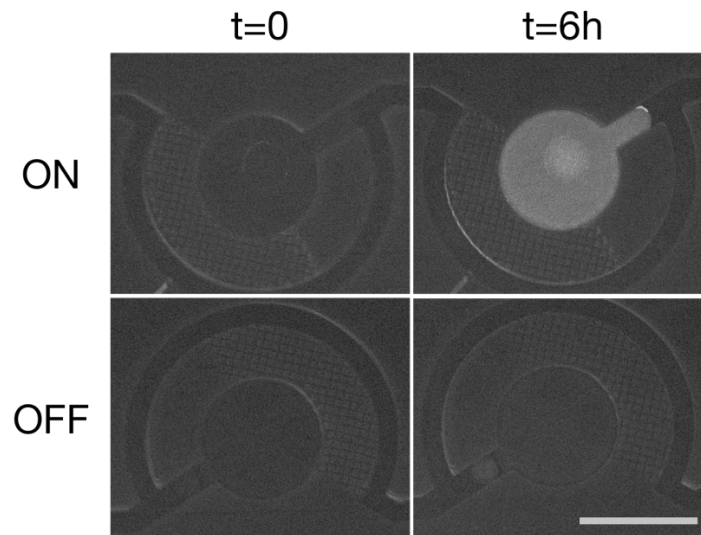

Figure 10. S30 S30 3OC6-HSL communication inside the dialysis chip. *The dialysis chip was mounted with the Teflon foil partially aligned with the storage layer. As a result, some of the circular wells of the storage layer were not in contact with the reservoir layer. A S30 reaction was supplemented with the receiving template BBa_T9002 and loaded in the circular well. A S30 reaction was supplemented with the sending construct MC002A and loaded on the reservoir layer of the dialysis chip. A flow rate of 5 μL/hour was set at 25 °C. Shown are pictures taken after 6 hours of incubation. Two examples of ON and OFF wells are shown right after the chip loading and the final timepoint. Scale bar: 400 μm.*

4.3. Discussion

The dialysis device described in this work is an adaptation of the one designed and developed by Kornreich and colleagues[24]. Here the dialysis device is composed by two microfluidic chips that differ not only in the features design but also in the material composition.

PDMS was used to cast the lower layer (storage layer) while polypropylene was molded to create the upper layer (reservoir layer). This chapter reports the preparation and characterization of the polypropylene chip, while the casting of PDMS chips has already been shown. Polypropylene was shaped by heat incubation. The use of PDMS as mold is suited for two reasons. First, PDMS can tolerate high temperatures therefore it will not degrade in the heating step necessary for polypropylene softening and shaping. Second, after the cooling of the plastic, PDMS can be peeled off the polypropylene chip.

The aqueous sample loaded in the upper layer fills the wells of the polypropylene chip. By carefully adjusting the Teflon foil at the interface between the storage layer and the reservoir layer, it is possible to prevent some wells to be aligned with the hole in the foil. Such OFF-wells cannot communicate with the reservoir layer across the dialysis membrane in the chip. To avoid crosstalk, ON and OFF wells need to be carefully separated. To this end, oil is flushed behind the aqueous sample. Aqueous sample will not exit from the wells thanks to the small pillars design which exploits the high Laplace pressure of water samples. To make the process possible, a stable interface must be created between the aqueous sample and the oil. A fluorinated oil was used for the separation of the wells and a biocompatible fluorinated surfactant was found to be suited for the stabilization of the interface.

Biochemical communication among engineered *E. coli* bacteria was carried out in the dialysis chip as a proof-of-concept experiment. Likewise, the same communication experiment was performed in a completely cell-free manner, using a homemade transcription-translation system. The apparatus was therefore shown to be functional and suited for studies involving the diffusion of small molecules across a dialysis membrane. Moreover, the total volume of all the 100 nanoliter-size wells of the storage layer is approximately 1 μL, thus allowing the use of less resources. Chemical communication

carried out inside the dialysis chip can be useful for the rapid prototyping and test of genetic circuits or the individual characterization of uncultured microorganisms which growth is dependent on specific factors provided by co-existing symbionts. Such microorganisms fail to survive on petri dishes but could proliferate in the microfluidic chip wells if put in contact with the mother soup on the reservoir compartment. Proper dilution of the sample would ensure the statistical distribution of one cell per well. Each one of these different microbes would be free to exchange factors with the mother soup stored in the reservoir while growing in an isolated compartment and forming homogeneous colonies to be recovered and used for downstream analyses.

4.4. Materials and methods

Note. Design of the chips and fabrication of the silicon wafer molds are procedures credited to and performed by Michael Heymann and Thomas Perli.

Mask design and silicon mold fabrication

The different layers of the chip were designed using AutoCAD software. In total, one storage design and four different reservoir designs were adopted.

The storage layer is characterized by a bypass serpentine connecting 100 round shaped wells with diameters of 400 µm (Figure 11). This design is a two-layer layout and for this reason two masks are needed. The bypass channel and well heights are equal to the sum of the first and the second photoresists layers. The small pillar array height is equal to the second layer of photoresist. The files were printed on a transparency film using a high-resolution printer. The transparencies were used as masks for the photolithography.
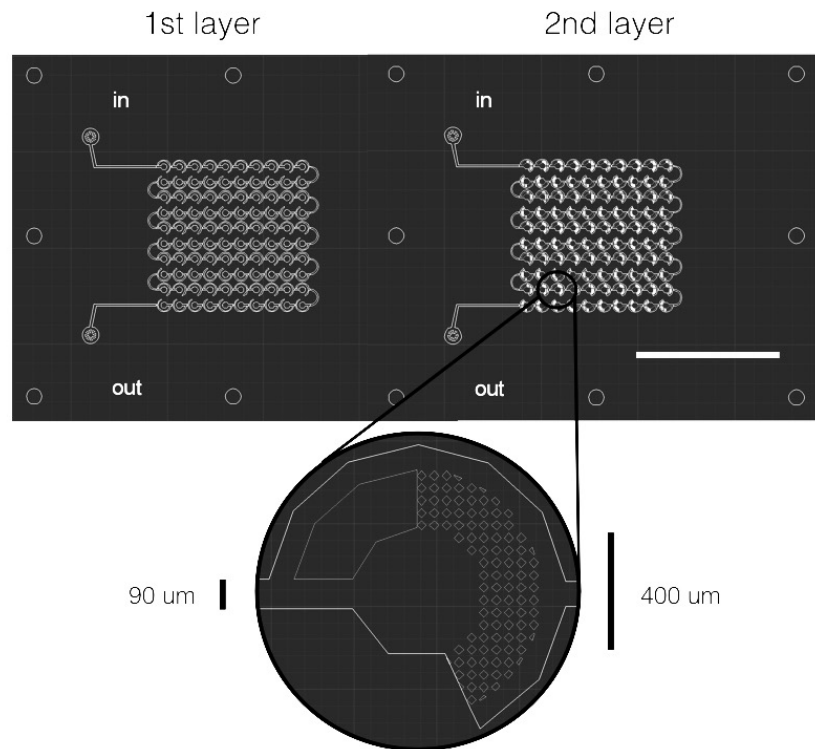
Figure 11. AutoCAD designs for the storage layer. *On the left, the first mask is presented with transparencies for the lithography of the wells and the bypass channel. On the right, the second mask for the lithography of the second layer of photoresist is shown. The second mask also contains the features for creating the pillar array acting as valve for retaining the water sample (light features). Scale bar = 10 mm.*

The reservoirs were simply a perfusion system characterized by four parallel serpentines in order to avoid collapsing of the structure (Figure 12).
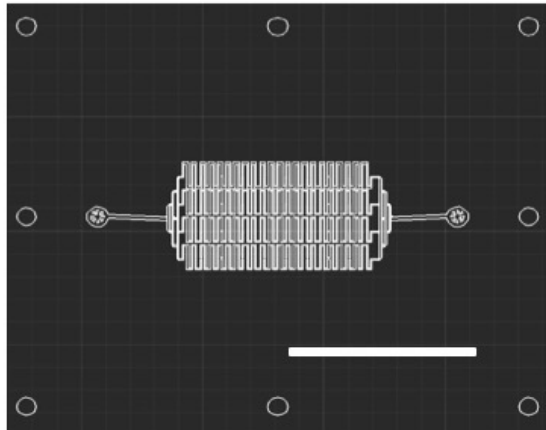
Figure 12. AutoCAD design for the reservoir chip. *A single mask was used for the photo-lithography of the reservoir silicon mold. The design presents four parallel serpentines creating a walls pattern to prevent collapse of the structure. Scale bar = 10 mm.*

Master molds were prepared by standard photo-lithography technique in a cleanroom (Figure 13). For the storage layer, two different SU-8 (MicroChem) resist layers were applied on the silicon wafer to obtain a two-layer negative of the chip design. The silicon wafer was cleaned and a drop of SU-8 was applied in the middle of the silicon wafer and spin coating was performed following manufacturer guidelines to obtain an approximate height of 100 μm[27]. The wafer was soft baked on a hot plate at 95°C in order to evaporate the solvent. The SU-8 film was exposed to UV light through the mask using an aligning machine. A post-exposure bake was performed to selectively cross-link the UV-exposed portion of the film. The process was repeated to create the second layer of SU-8 photoresist using the second mask. Finally, the non-exposed photoresist was removed from the wafer by dipping into propylene glycol monomethyl ether acetate (PGMEA) solvent for 5 min. An extra isopropanol rinse was performed to ensure the complete removal of non-exposed photoresist, being non-crosslinked SU-8 insoluble in isopropanol and becoming visible as white mesh.
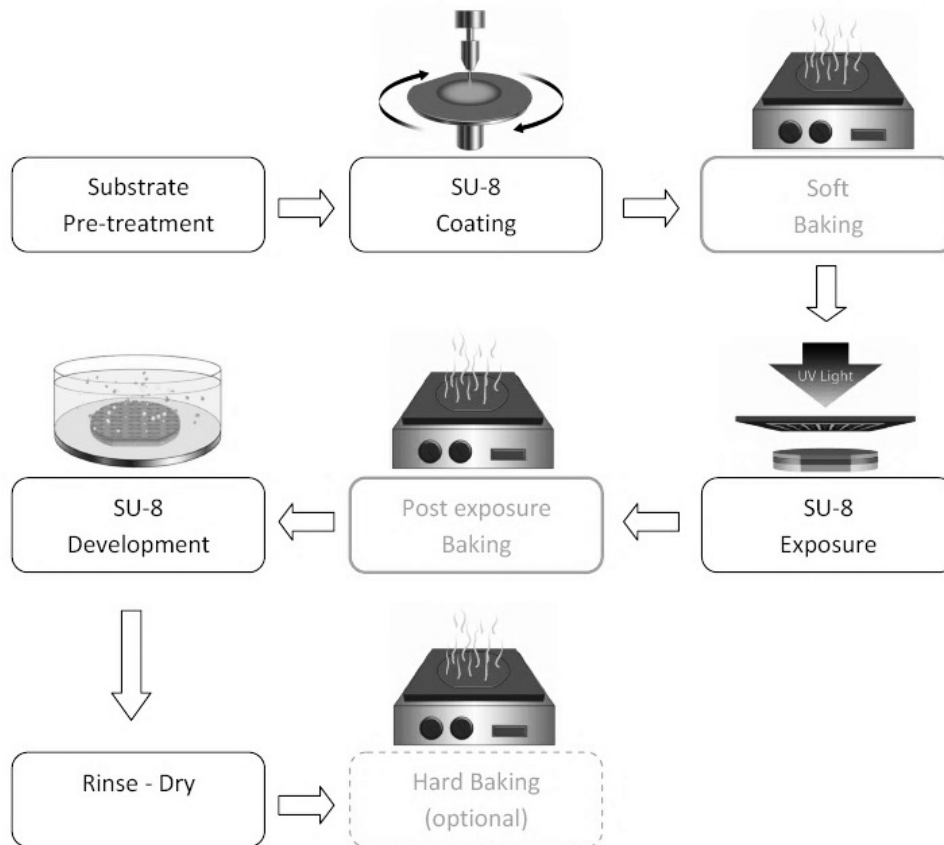
Figure 13. Schematic representation of the master mold fabrication protocol.
To obtain a multilayer structure, SU-8 Coating through to Post exposure Baking steps
are repeated using a mask for the next photoresist layer UV crosslinking[28].

PDMS chip casting and preparation

To prepare the PDMS chips, Sylgard® 184 silicone elastomer kit (Dow Corning) was used. The dust was removed from the features of the silicon wafer using N_2 high pressure flow and placed in a petri dish previously covered with aluminum foil. About 20 g of PDMS pre-resin and 2 g of curing agent (10% w/w) were mixed and mixed in a plastic beaker using a pipette tip. The resin was poured on top of the wafer and incubated in a vacuum desiccator. Vacuum was applied for 30 min in order to remove all of the air bubbles from the resin. PDMS was cured at 70 °C, 40 min. Using a scalpel, the PDMS slab was cut and peeled from the mold (Figure 14). Inlet and outlet holes were created with a biopsy puncher (World Precision Instruments). Since the PDMS layers had to be assembled as a sandwich, holes were created from the side.

Figure 14. Schematic representation of PDMS chip casting. PDMS polymer, mixed with curing agent, is poured on top of the silicon wafer and cured at 40-80 °C for 40 minutes. The cured PDMS is cut and peeled off the mold, ready to use. The silicon wafer mold can be used for countless PDMS chip casting.

Polypropylene chip printing and preparation

Polypropylene is classified as a polyolefin and is a high-molecular weight hydrocarbon. Like all polyolefins, polypropylene is a non-toxic, non-contaminating, very inert and hydrophobic materials, which does not degrade in contact with biological samples. Moreover, polypropylene has no known solvent at room temperature. Because of these highly favorable features, polypropylene is virtually found in every molecular and cellular biology laboratory as the most common material for each kind of plasticware.

Figure 15. Schematic representation of polypropylene chip preparation. The polypropylene chip is softened by heat and pressed against a PDMS chip that acts as mold and allows for the printing of the chip features on the plastic. The PDMS mold is casted on a reverse-featured silicon wafer. The PDMS mold can be used for several polypropylene chip preparations.

A hydrophobic coating was performed for the polypropylene storage chip. After cleaning the chip features with tape, the surface was treated with Easytreat BC20 Mini corona treater (Boussey Control) for 15-30 seconds, keeping the electrode at 2 cm from the chip. 10 µL of a solution of 1.5 g Cytop 809M and 25 g Solv 100E (AGC Chemicals) were poured on top of the features. Cytop is an amorphous (non-crystalline) fluoropolymer that is transparent and allows for thin film coating of different surfaces. Cytop treatment was completed by incubation of the polypropylene chip at 70 °C, 2 hours.

Dialysis chip assembly

The dialysis chip is composed of a polypropylene storage layer and a PDMS reservoir layer facing one another and separated by a cellulose dialysis membrane (Spectra Labs) and a fluorinated ethylene propylene (FEP, Teflon) foil (McMaster Carr). The Teflon foil is ca. 50 μm thick and acts as a wetting control layer. The foil was cut using a VLS3.50 Versa laser cutter with 50 W Imaging Cartridge with High Power Density Focusing Optics (HPDFO) to obtain holes of about 200 μm in diameter. The sandwich is kept together by two metal frames with tightening screws.

Before starting the assembly, all parts are cleaned: glass slides with ethanol while PDMS parts with adhesive tape and pressurized air. Chip inlets and outlets are connected with 300 μm inner diameter #30 AWG poly(tetrafluoroethylene) tubing (PTFE) tubing (Cole Palmer). To assemble the chip, a glass slide is placed inside one frame and the reservoir layer is placed in the center with features up. The dialysis membrane is hydrated in water and then placed on top of the reservoir chip. The FEP foil is then put on top of the membrane and the polypropylene storage layer is placed, features down, on top of the foil, paying attention to align the holes to obtain one hole in each round well. Alignment of polypropylene storage chip and Teflon foil is performed using a stereomicroscope. A glass slide followed by the second metal frame are placed on top of the layers and the sandwich is tightened with screws. Since PDMS is an elastomer, features can be deformed if the pressure is too high. On the other hand, the chip needs to be enough tightened in order not to have leaks.

Storage layer loading

The storage layer design allows for loss-free sample loading using capillary valving. Samples are loaded in round wells that are connected in series by a continuous serpentine through which one well is loaded after the other. To eliminate sample loss from channel dead volume, the capillary valve based "store-then-create" loading technique is exploited[29]. The chip is primed with HFE-7500 oil by flowing the oil from the chips outlet in order to remove air bubbles. A 100 μL gas-tight syringe with a luer-lock (SGE Analytical Science) is loaded with HFE-7500 oil and connected through a 18G needle to the PTFE tubing. The aqueous sample is then sucked into the tubing and the syringe is

connected to a KDS100 syringe pump (KD scientific); a flow rate of about 10 µL/h is set. Once the sample starts moving, the tubing is connected to the storage chip inlet. The surface tension at the oil-water interface between priming oil and aqueous sample resulted in a pressure difference across the interface. This Laplace pressure can be calculated by the Young-Laplace equation as

$$\Delta P = \sigma \left(\frac{1}{Rx} + \frac{1}{Ry} \right)$$

where Rx and Ry are the main radii of curvature and σ is the surface tension of the interface. To minimize its energy, the oil-sample interface has to minimize its surface which is equivalent to maximizing its main radii of curvature at constant volume. A low curvature interface in a wide channel has a lower Laplace pressure then a high curvature interface in a narrow channel segment. Therefore, the sample plug preferentially entered and flowed through the wide bypass channel instead of flowing through the narrow capillary valve channel (green section, Fig.8). The sample plug was then followed again by oil, which separated the sample in the wells into independent droplets.

Dialysis chip in vivo 3OC6-HSL sending and receiving

BL21 (DE3) Singles (Novagen) were transformed with sending (BBa_T9002) or receiving (MC002A) plasmid vectors and spread onto LB agar plates supplemented with 50 µg/mL ampicillin. Single colonies were picked and used to start overnight cultures in LB with 50 µg/mL ampicillin at 37 °C, 220 rpm. Overnight cultures were diluted 100-fold in fresh LB with ampicillin and grown till $OD_{600 \, nm} = 0.5$ at 37 °C, 220 rpm. The sending culture was induced with 0.5 mM IPTG and incubated 1 hour at 37 °C, 220 rpm. The dialysis chip was assembled with the storage layer partially aligned with the Teflon foil. In this way, some of the wells were located over a part of the Teflon foil lacking the hole and thus, the communication with the lower layer was prevented. These wells were supposed to constitute the negative control in which 3OC6-HSL produced by the sending *E. coli* could not reach the receiving bacteria. A sample from the receiving culture was loaded on a 100 µL gas-tight syringe (SGE Analytical Science) and dispensed in the storage upper layer through PFTE tubing connected to the syringe needle. Oil was flushed right after the sample to isolate the wells. Once every well was containing the sample and

the oil filled the channels, the oil syringe was connected to a KDS100 syringe pump (KD scientific) and a constant flow of 5 µL/hour was set. A sample from the sending culture was loaded on the lower reservoir layer with another syringe and a constant flow of 5 µL/hour was set using another syringe pump. Images of the loaded dialysis chip were acquired using an inverted Primovert iLED microscope (Zeiss).

4.5. References

1.   Lee, S. H. *et al.* Capillary Based Patterning of Cellular Communities in Laterally Open Channels. *Anal. Chem.* **82,** 2900–2906 (2010).

2.   Berry, S. M., Maccoux, L. J. & Beebe, D. J. Streamlining Immunoassays with Immiscible Filtrations Assisted by Surface Tension. *Anal. Chem.* **84,** 5518–5523 (2012).

3.   Anna, S. L., Bontoux, N. & Stone, H. A. Formation of dispersions using flow focusing'' in microchannels. doi:10.1063/1.1537519

4.   Van Lintel, H. T. G., Van De Pol, C. M. & Bouwstra, S. A PIEZOELECTRIC MICROPUMP BASED ON MICROMACHINING SILICON OF. *Sensors and Actuators* **15,** 153–167 (1988).

5.   Harrison, D. J., Manz, A., Fan, Z., Luedi, H. & Widmer, H. M. Capillary electrophoresis and sample injection systems integrated on a planar glass chip. *Anal. Chem.* **64,** 1926–1932 (1992).

6.   Aumiller, G. D., Chandross, E. A., Tomlinson, W. J. & Weber, H. P. Submicrometer resolution replication of relief patterns for integrated optics. *J. Appl. Phys.* **45,** 4557–4562 (1974).

7.   Masuda, S., Washizu, M. & Nanba, T. Novel method of cell fusion in field constriction area in fluid integration circuit. *IEEE Trans. Ind. Appl.* **25,** 732–737 (1989).

8.   David C. Duffy, J. Cooper McDonald, Olivier J. A. Schueller, and & Whitesides*, G. M. Rapid Prototyping of Microfluidic Systems in Poly(dimethylsiloxane). (1998). doi:10.1021/AC980656Z

9.   Berthier, E., Young, E. W. K. & Beebe, D. Engineers are from PDMS-land, Biologists are from Polystyrenia. *Lab Chip* **12,** 1224 (2012).

10.   Goral, V. N., Hsieh, Y.-C., Petzold, O. N., Faris, R. A. & Yuen, P. K. Hot embossing of plastic microfluidic devices using poly(dimethylsiloxane) molds. *J. Micromechanics Microengineering* **21,** 17002 (2011).

11.   Wang, Y. *et al.* Benchtop micromolding of polystyrene by soft lithography. *Lab Chip* **11,** 3089 (2011).

12.   Young, E. W. K., Berthier, E. & Beebe, D. J. Assessment of enhanced autofluorescence and impact on cell microscopy for microfabricated thermoplastic devices. *Anal. Chem.* **85,** 44–9 (2013).

13.   Martinez, A. W., Phillips, S. T. & Whitesides, G. M. Three-dimensional microfluidic devices fabricated in layered paper and tape. *Proc. Natl. Acad. Sci.* **105,** 19606–19611 (2008).

14.   Pardee, K. *et al.* Paper-Based Synthetic Gene Networks. *Cell* **159,** 940–954 (2014).

15.   Zhou, J., Ellis, A. V. & Voelcker, N. H. Recent developments in PDMS surface modification for microfluidic devices. *Electrophoresis* **31,** 2–16 (2010).

16.   Unger, M. A., Chou, H. P., Thorsen, T., Scherer, A. & Quake, S. R. Monolithic microfabricated valves and pumps by multilayer soft lithography. *Science* **288,** 113–6 (2000).

17.   Thorsen, T., Maerkl, S. J. & Quake, S. R. Microfluidic Large-Scale Integration. *Science (80-.).* **298,** 580–584 (2002).

18.   Regehr, K. J. *et al.* Biological implications of polydimethylsiloxane-based microfluidic cell culture. *Lab Chip* **9,** 2132 (2009).

19.   Toepke, M. W. & Beebe, D. J. PDMS absorption of small molecules and consequences in microfluidic applications. *Lab Chip* **6,** 1484 (2006).

20.   Heo, Y. S. *et al.* Characterization and Resolution of Evaporation-Mediated Osmolality Shifts That Constrain Microfluidic Cell Culture in Poly(dimethylsiloxane) Devices. *Anal. Chem.* **79,** 1126–1134 (2007).

21.   Young, E. W. K. *et al.* Rapid Prototyping of Arrayed Microfluidic Systems in Polystyrene for Cell-Based Assays. *Anal. Chem.* **83,** 1408–1417 (2011).

22.   Khnouf, R., Olivero, D., Jin, S., Coleman, M. A. & Fan, Z. H. Cell-Free Expression of Soluble and Membrane Proteins in an Array Device for Drug Screening. *Anal. Chem.* **82,** 7021–7026 (2010).

23. Timm, A. C., Shankles, P. G., Foster, C. M., Doktycz, M. J. & Retterer, S. T. Toward Microfluidic Reactors for Cell-Free Protein Synthesis at the Point-of-Care. *Small* **12,** 810–817 (2016).

24. Kornreich, M., Heymann, M., Fraden, S. & Beck, R. Cross polarization compatible dialysis chip. *Lab Chip* **14,** 3700–4 (2014).

25. Holtze, C. *et al.* Biocompatible surfactants for water-in-fluorocarbon emulsions. *Lab Chip* **8,** 1632 (2008).

26. Stevens, A. M., Fujita, N., Ishihama, A. & Greenberg, E. P. Involvement of the RNA polymerase alpha-subunit C-terminal domain in LuxR-dependent activation of the Vibrio fischeri luminescence genes. *J. Bacteriol.* **181,** 4704–7 (1999).

27. Micro Chem. Soft Bake Substrate Pretreatment. Available at: http://www.microchem.com/pdf/SU8_50-100.pdf. (Accessed: 3rd February 2018)

28. Elveflow. Soft Lithography: SU-8 baking - Elveflow. Available at: https://www.elveflow.com/microfluidic-tutorials/soft-lithography-reviews-and-tutorials/how-to-get-the-best-process/soft-lithography-su-8-baking/. (Accessed: 3rd February 2018)

29. Boukellal, H., Selimović, Š., Jia, Y., Cristobal, G. & Fraden, S. Simple, robust storage of drops and fluids in a microfluidic device. *Lab Chip* **9,** 331–338 (2009).

Conclusions and future perspectives

The aim of this work was the reconstitution of cell-free protein synthesis systems and the exploration of possible applications. Despite the PURE system was reconstituted and showed to be working, the activity of the system was very low compared to the commercially available kit. The second approach for the preparation of the PURE system in which protein pools are obtained from engineered strains, yielded a more active cell-free protein synthesis system. Also in this case some considerations must be taken. The advantage of using a protein synthesis kit reconstituted from purified components relies on the possibility of adjusting every single part of it. The PURE system reconstitution using enzymes pools instead of singularly purified proteins significantly reduces the amount of work but yields a less flexible system in which the concentration of specific components cannot be adjusted. In this sense, the second preparation is easier but the product lacks the fundamental characteristic of the PURE system *i.e.* the complete control over each and every one component inside the mix. The S30 *E. coli* cellular Extract on the other hand comes as a "black-box" by definition. The S30 Crude Extract is a highly heterogeneous mix which include among the others all the components for protein synthesis. Every output of this system must therefore be interpreted accordingly, also considering that protein expression reactions carried out with S30 Extract may better simulate what actually happens in living bacteria, given the presence of virtually every protein synthesis-related component. To improve the activity of the PURE system, a fine tuning of all the components should be carried out. Also, a test of activity for the tRNA synthetases can be introduced in order to minimize possible sources of malfunctioning of the system.

Commercial PURE system and homemade S30 Extract were used in an attempt to characterize the variability of transcription and translation *in vitro*. Evidences are provided suggesting that *in vitro* translation is more variable than transcription. The complexity of the process and the number of components involved in translation are probably the most accounting factors. In fact, variability in mRNA synthesis in S30 Extract decreased by switching from *E. coli* RNA polymerase- to T7 RNA polymerase-driven transcription, consistent with the fact that higher grades of complexity (see *E. coli*

vs T7 RNA polymerases) are related with higher output variability. The secondary structures in which RNA can fold are also clearly involved in the efficiency of protein synthesis. Using synonymous sequences with lower GC content in the commercial PURE system led to a higher protein/mRNA ratio, suggesting a more efficient use of the available mRNA. It is important to say that the reporter gene used in this study is a fluorescent protein. Quantification with different methods and expression of an enzyme to be tested in an assay would provide significant information on how different GC content in the mRNA sequence could affect the protein output functionality. The influence of RNA folding on protein synthesis may be further investigated. The approach of testing the effect of GC content on translation can be extended to other proteins. To additionally get insights on what mediates the effect of RNA folding, the PURE system and the S30 Extract should always be compared. Extracts should contain every translation-related factor therefore divergences between the two *in vitro* transcription systems are expected. Differences may be reduced with the addition of specific factors to the PURE system or with the use of chaotropic agents to minimize the effect of RNA folding on translation. Lower GC content effect may be also investigated in un-coupled protein synthesis. Providing an mRNA template to cell-free expression systems leads to translation un-coupled with transcription. The lower efficiency of the system is thought to be due to secondary structures formation and resulting lower accessibility of the transcript for ribosomes. According to the observations presented in this work, a partial recovery of un-coupled translation efficiency would be expected.

In order to characterize one of the steps of a proposed network involving artificial and natural cells, the activity of pore forming proteins was tested on calcein encapsulating liposomes. The S30 Extract was used as platform for *in vitro* expression of the pore forming proteins and at the same time, the goodness of the proposed expression regulation system was assessed. Among the three pore forming proteins tested, PFO is the most active in permeabilization. This study lacks an estimation of the encapsulation efficiency of the liposomes prepared. Regardless, among the different liposomes tested, the most suited for permeabilization are the ones with the higher cholesterol content present in the membrane. The expression regulation control based on the *quorum sensing* molecule 3OC6-HSL is not tight enough, providing a basal level of the gene of interest even in absence of the inducer. Therefore, a new regulation circuit involving T7 RNA polymerase

was tested *in vivo*. *E. coli* bacteria transformed with the plasmid constructs could successfully permeabilize liposomes showing that the system is functional. Permeabilization was observed after overnight incubation of induced bacteria with liposomes. Although this result indicates a good stability of the liposomes, it also implies that the downstream steps of the communication network will be delayed. To eventually test if the complete network communication is functional, all the components have to be put together and the final output of the communication flow, that is the killing of a population of reporter-expressing *E. coli* bacteria, assessed.

A microfluidic device was developed for the exchange of water-soluble small molecules between low volume samples across a dialysis membrane. Applications of the dialysis device range from testing of chemical communication to cell-free protein synthesis reaction prototyping. The preparation of one of the two layers of the chip was characterized. The chosen material was polypropylene because of its more rigid structure compared to PDMS. This biocompatible plastic was softened by heat and successfully shaped on a PDMS mold. The resulting polypropylene chip showed to be optimal for the dialysis chip mounting and chemical communication between two bacteria populations was established. Communication inside the chip involving bacteria and cell-free protein synthesis reactions was shown. *In vitro* protein synthesis in the dialysis chip may establish a platform for the testing of cell-free systems which are meant to be eventually encapsulated for the creation of communicating artificial cells. In case of artificial entities to natural cells communication but also if testing artificial cells to artificial cells communication, the dialysis device could serve as an assaying platform. In fact, the chip features permit a physical separation of the samples while allowing the exchange of small water-soluble molecules through the dialysis membrane. This setting could mimic and act as a compartment for the early stages of the setting of an artificial cell system in order to avoid the preparation of the actual cell-like compartment every time a new part has to be evaluated. Moreover, the device can be used to isolate and grow uncultured microorganisms which need the exchange of soluble factors with the members of a community. Eventually, homogeneous cultures could be recovered for downstream characterization.

Appendix

Plasmid constructs table

Name	Backbone	Insert
DC032A	pET21b	pT7_trpO_ mRFP1_spinach
DC076A	pET21b	pT7_trpO_ mRFP1_spinach _pT7_TrpR
DC129A	pET21b	pTac_B0034_mRFP1_MGapt
DC171A	pET21b	pT7 - lacO - PFO - T7term - pT7 - lacO - ColE7
DC174C	pACYC184	pTet - luxR - rrnBT1 - pluxR - T7RNApol - rrnBT1 - pTet - T7lysozyme
FC001A	pUC57	pT7 - MGapt
FC045A	pET21b	pT5 - lacO - mRFP1 - spinach
GB002A	pET21b	pT5 - lacO - 6xHis - T7RNApol
GB008A	pET21b	pTac_B0034_mRFP1_pRNA with MGapt
NT001A	pET21b	pT7 - lacO - aHL - T7term - pT7 - lacO - ColE7
NT002A	pET21b	pT7 - lacO - LLO - T7term - pT7 - lacO - ColE7
pVS10		pT7 - lacO - rpoA - rpoB - rpoC - 6xHis
pIA586		pT7 - lacO - rpoD - 6xHis
BBa_T9002		pTet - luxR - rrnBT1- pluxR - GFPmut3b
MC002A	pET21b	pT7 - LuxI

Peer-reviewed Publication

Cell-free translation is more variable than transcription

Fabio Chizzolini, Michele Forlin, Noël Yeh Martín, **Giuliano Berloffa**, Dario Cecchi, & Sheref S. Mansy.

ACS Synthetic Biology, 2017

doi: 10.1021/acssynbio.6b00250 (19 January 2017).

Manuscript in preparation

A microfluidic dialysis device for bacterial and cell-free chemical communication

Giuliano Berloffa, Thomas Perli, Michael Heymann, Petra Schwille, Sheref S. Mansy

Acknowledgements